

# The *Wnt/β-catenin/TCF/Sp5/Zic4* gene network that regulates head organizer activity in *Hydra* is differentially regulated in epidermis and gastrodermis

Laura Iglesias Ollé<sup>1</sup>, Chrystelle Perruchoud<sup>1</sup>, Paul Gerald Layague Sanchez<sup>1</sup>, Matthias Christian Vogg<sup>1</sup> and Brigitte Galliot<sup>1,\*</sup>

<sup>1</sup> Department of Genetics and Evolution, Institute of Genetics and Genomics (iGE3), Faculty of Sciences, University of Geneva; 30 Quai Ernest Ansermet, 1211 Geneva 4, Switzerland;  
\* Correspondence: brigitte.galliot@unige.ch

**Abstract:** In *Hydra*, head formation depends on *Wnt/β-catenin* signaling, which positively regulates *Sp5* and *Zic4*, with *Sp5* limiting *Wnt3/β-catenin* expression and *Zic4* triggering tentacle formation. Using transgenic lines in which the *HySp5* promoter drives eGFP expression in the epidermis or gastrodermis, we show that in intact animals, epidermal *HySp5:GFP* is expressed strongly apically and weakly along the body column, while gastrodermal *HySp5:GFP* is also maximally expressed apically but absent from the oral region, and remains high along the upper body column. During apical regeneration, gastrodermal *HySp5:GFP* appears early and diffusely, epidermal *HySp5:GFP* later. Upon alsterpaullone treatment, apical *HySp5:GFP* expression is shifted to the body column where epidermal *HySp5:GFP* transiently forms ectopic circular figures. After *β-catenin*(RNAi), only epidermal *HySp5:GFP* is down-regulated, while pseudo-bud structures expressing gastrodermal *HySp5:GFP* develop. *Sp5*(RNAi) highlights the negative autoregulation of *Sp5* in epidermis, involving direct binding of *Sp5* to its own promoter as observed in human HEK293T cells. In these cells, *HyZic4*, which can interact with *hTcf1*, regulates *Wnt3* negatively and *Sp5* positively. This differential regulation of the *Wnt/β-catenin/TCF/Sp5/Zic4* network in epidermis and gastrodermis highlights distinct architectures and patterning roles in the hypostome, tentacle and body column, as well as distinct regulations in homeostatic and developmental organizers.

**Keywords:** *Hydra* head organizer; *Hydra* transgenic lines; epidermal and gastrodermal epithelial layers; *Sp5* transcription factor; *Sp5* promoter autoregulation; *Zic4* transcription factor; *Zic4* tentacle regulator; *Wnt/β-catenin* signaling; gene regulatory network (GRN); HEK293T mammalian cells;

## 1. Introduction

*Hydra* is a freshwater hydrozoan polyp known for its exceptional regenerative capacities, able to regrow any missing part of its body, such as a new fully functional head in three to four days after mid-gastric bisection (reviewed in [1]). Its anatomy is simple, basically a gastric tube composed of two myoepithelial layers known as the epidermis and gastrodermis along a single oral-aboral axis (Figure 1A). This bilayered gastric tube connects the apical or head region at the oral side, to the basal disc at the aboral side. The regenerative process relies on the rapid establishment of a head organizer in the regenerating tip, initially identified by Ethel Browne through transplantation experiments [2]. Indeed, she showed that tissues isolated from the head of intact animals, from the head-regenerating tip or from the presumptive head of the developing bud, can instruct and recruit cells from the body column of the host to induce the formation of an ectopic head, a property later named *organizer activity*. Additional transplantation experiments confirmed that the head organizer is actively involved in *developmental processes* in *Hydra* such as 3D reconstruction of the missing head after decapitation at any level along the body column or formation of a new head during budding. In addition, the head organizer is

also required in a *homeostatic context*, actively maintaining head patterning in intact animals [3–8]. Hence, in *Hydra*, two types of head organizer activity take place, one in homeostasis and the other in developmental contexts, the latter ones giving rise to the former.

The principle of *organizer activity* was later shown to be also at work during embryonic development in vertebrates, initially in gastrulae [9,10] and later on during appendage and hindbrain development [11–14]. These organizers are transient developmental structures with evolutionarily conserved patterning properties [15]. Similarly, regenerating blastema that form after amputation can be considered as organizing centers, which exhibit patterning properties to reconstruct the missing structure due to the molecular instructions they deliver to the surrounding cells to modify their behavior [16–18,7]. Indeed, these recruitment and patterning properties can be observed by transplanting regenerative blastema.

The *Hydra* polyp, an animal easily maintained in the laboratory, provides a model to decipher the cellular and molecular basis of regeneration. Transplantation experiments identified two distinct activities for the head organizer named head activation and head inhibition, both with maximal activity apically and a theoretical parallel apical-to-basal graded distribution along the body axis [19,20,4,6]. In 1972, Gierer and Meinhardt proposed a Turing's derived reaction-diffusion model to predict how the organizer is acting and how it gets reestablished after bisection, both processes relying on the cross-talk between a short range activator and a longer range inhibitor acting in a positive-negative feedback loop [21]. According to this model, the activator positively acts on its own production as well as on that of the inhibitor, whereas the inhibitor negatively acts on production/activity/stability of the activator. In any position along the animal length, the balance between these two components is tightly controlled under homeostatic conditions, but immediately disrupted upon amputation, resulting in rapid restoration of the activity of the activating component, i.e. head activation, and delayed restoration of the activity of the inhibitory component, i.e. head inhibition, given their respective rates of diffusion, self-regulatory capacity, and cross-regulation.

Three decades later, Wnt/β-catenin signaling was proposed to actually act as the head activator, required to initiate apical morphogenesis and maintain apical differentiation in *Hydra* [22–27]. More recently, the transcription factor Sp5, whose expression is regulated by Wnt/β-catenin signaling in many species including *Hydra* [28–33], was shown to restrict the activity of Wnt/β-catenin signaling, thus fulfilling the expected positive-negative feedback loop of the head inhibitor [33]. Indeed, a transient knock-down of *Sp5* suffices to induce a multiheaded phenotype characterized by ectopic head formation along the body column of intact animals and regeneration or budding of animals with multiple heads [33]. As anticipated, after mid-gastric bisection, *Sp5* and *Wnt3* are up-regulated in the apical-regenerating tips, within two to three hours for *Wnt3*, after eight hours for *Sp5*, and both of them remain expressed at high levels throughout the entire head regenerative process but not the foot one [33]. Also, the transcription factor Zic4, whose gene expression is positively-regulated by *Sp5*, is responsible for the maintenance of tentacle differentiation and for their formation during apical development [34].

*Hydra* is populated by a dozen distinct cell types that derive from three adult stem cell populations, i.e. epithelial epidermal, epithelial gastrodermal and interstitial, which constantly self-renew in the body column to maintain *Hydra* homeostasis. In intact animals, *Wnt3*, *Sp5* and *Zic4* are predominantly expressed in epithelial cells of both gastrodermis and the epidermis [25,33,34], a finding confirmed by single-cell sequencing [35] (**Figure S1**). However, while *Wnt3*, *Sp5* and *Zic4* are expressed at highest levels apically, their respective profiles in the apical region are very different: *Wnt3* is detected at a maximum level at the tip of the head, around the mouth opening, where the organizing activity is located [25,27]. In this region, *Sp5* and *Zic4* are in fact not detected, their expression being maximal at the base of the head where the tentacles are implanted and in the proximal region of the tentacles. Also, *Sp5* is the only one to be detected along the body column.

Pharmacological and genetic manipulations have shown that dynamic interactions between Wnt/β-catenin, Sp5 and Zic4 play a crucial role for apical development and maintenance of apical patterning [33,34]. However, although *Wnt3* is predominantly expressed in the gastrodermis, the specific role of each epithelial layer in the formation and maintenance of the head organizer remains unknown. The aim of this study is to uncover the dynamics of the Wnt/β-catenin/Sp5/Zic4 gene regulatory network in the epidermis and gastrodermis. To test these regulations in homeostatic and developmental contexts, we generated two transgenic lines that constitutively express the *HyAct-1388:mCherry\_HySp5-3169:GFP* reporter construct in either epithelial layer. We monitored mCherry and GFP fluorescence in parallel with the detection of *GFP*, *Sp5*, *Wnt3* expression in intact, budding or regenerating animals, as well as in animals where Wnt/β-catenin signaling is either stimulated or knocked-down. In each of these contexts, we recorded distinct regulations of *Sp5* in the epidermis and gastrodermis, notably an epidermal-specific negative autoregulation of *Sp5* in the body column. These results point to distinct architectures of the Wnt/β-catenin/Sp5/Zic4 gene regulatory networks active in the epidermis and the gastrodermis, and we discuss their respective roles in the regulation and activity of the head organizer.

## 2. Materials and Methods

### 2.1. Animal culture and drug treatment

*Hydra vulgaris* (*Hv*) from the *Basel* (*Hv\_Basel*), *magnipapillata* (*Hm-105*) or *AEP2* (*Hv\_AEP2*) strains [36] were cultured in Hydra Medium (HM: 1 mM NaCl, 1 mM CaCl<sub>2</sub>, 0.1 mM KCl, 0.1 mM MgSO<sub>4</sub>, 1 mM Tris pH 7.6) at 18°C and fed two to three times a week with freshly hatched *Artemia nauplii* (Sanders, Aqua Schwarz). For regeneration experiments, animals were starved for four days, then bisected at mid-gastric bisection. To activate Wnt/β-catenin signaling, *Hv\_Basel* or *Hv\_AEP2* animals starved for three or four days, were treated with 5 μM Alsterpaullone (ALP, Sigma-Aldrich A4847) or 0.015% DMSO for the indicated periods of time, and subsequently washed with HM.

### 2.2. Mapping of the transcriptional start sites (TSS)

*Sp5* and *Zic4* cDNAs sequences obtained by high throughput sequencing, available on [HydrAtlas](#) [37], Uniprot or NCBI were aligned to the corresponding *Hm-105* genomic sequences (**Table S1**) with the [Muscle Align](#) software ([ebi.ac.uk/Tools/msa/muscle/](http://ebi.ac.uk/Tools/msa/muscle/)) selecting a ClustalW output format. Next, the alignment was visualized with the [MView](#) tool [38] ([ebi.ac.uk/Tools/msa/mview/](http://ebi.ac.uk/Tools/msa/mview/)) and the putative TSS deduced from the 5' end of cDNAs.

### 2.3. Reporter constructs expressed in Hydra or in HEK293T cells

All reporter constructs used in this study are listed in **Table S3**. To produce the *HyAct-1388:mCherry\_HySp5-3169:eGFP* construct (further named *HySp5-3169:GFP*), a block of 3'194 bp *HySp5* sequences were amplified from *Hm105* genomic DNA including 2'968 bp promoter sequences, 201 bp 5'UTR sequences and 27 bp coding sequences. The sequences of the *HySp5* promoter Forward and Reverse primers are given in **Table S2**. The hoTG-*HyWnt3FL-EGFP-HyAct:dsRED* plasmid (kind gift from T. Holstein) [27] was then digested with the EcoRV and AgeI enzymes to remove the *HyWnt3FL* promoter region and insert the *Sp5* 3'194 bp region. Next, the dsRED sequence was replaced by the mCherry sequence by GenScript. The sequences of the final construct were verified by sequencing (**Figure S2**). From the *HySp5-2992:Luciferase* construct [33], six constructs were generated either by deleting the five Sp5-binding sites (BS) located in the proximal promoter or by mutating one of them: BS1 at position -129, BS2 at position -105, BS3 at position -52, BS4 at position -34, BS5 at position +18. These *HySp5-2828:Luc*, *HySp5-2992-mBS1:Luc*, *HySp5-2992-mBS2:Luc*, *HySp5-2992-mBS3:Luc*, *HySp5-2992-mBS4:Luc* and *HySp5-2992-mBS5:Luc* constructs were generated using the QuikChange Lightning Multi Site-Directed Mutagenesis Kit (Agilent Technologies).

#### 2.4. Generation of the Hydra transgenic lines

To generate the *Sp5* transgenic lines, gametogenesis was induced in *Hv\_AEP2* strain by alternating the feeding rhythm from four times per week to once a week consequently. The *HySp5-3169:GFP* construct was injected into one- or two-cell stage *Hv\_AEP2* embryos [39]. Out of 330 injected eggs, 27 embryos hatched and 3/27 embryos exhibited GFP and mCherry fluorescence. The epidermal and gastrodermal *HySp5-3169:GFP* lines analyzed in this work were obtained through clonal propagation from a single embryo for each of them in which only a few cells were positive after hatching. By asexual reproduction of the original animal, i.e. budding, we obtained two transgenic animals with a complete set of mCherry-eGFP positive epithelial cells, either epidermal or gastrodermal. The generation of the epidermal and gastrodermal *HyWnt3FL:eGFP-HyAct:dsRED* transgenic lines, renamed here epidermal *HyWnt3-2149:GFP* and gastrodermal *HyWnt3-2149:GFP*, is described in [33].

#### 2.5. RNA interference

For gene silencing experiments, we applied the procedure reported in [33]. Briefly, four-day starved budless animals were selected from the *Hv\_AEP2* culture, rinsed 3x in water, incubated for 45-60 minutes in Milli-Q water and electroporated with 4  $\mu$ M siRNAs, either targeting *Sp5* or  $\beta$ -catenin or scramble as negative control. For *Sp5* and  $\beta$ -catenin an equimolecular mixture of three siRNA was used (siRNA1+siRNA2+siRNA3, see sequences in **Table S2**). Animals were electroporated once, twice or three times (EP1, EP2, EP3) every other day as indicated.

#### 2.6. Quantitative RT-PCR

At indicated time-points after electroporation, 20 animals per condition were amputated either at 80% level to obtain the apical region (100%-80%) and the body column (80%-0%), or at 80% and 30% levels to obtain the apical region as above, the central body column (80%-30%) and the basal region (30%-0%). Beside electroporated transgenic animals, non-electroporated wild type *Hv\_AEP2* animals were used to provide the reference expression levels. The different parts of the animals were transferred to RNA-later (Sigma-Aldrich R0901) immediately after amputation and kept at 4°C prior to RNA extraction. RNA extraction was performed using the E.Z.N.A.® Total RNA kit (Omega) and cDNA was synthesized with the qScript™ cDNA SuperMix (Quanta Biosciences). The cDNA samples were diluted to 1.6 ng/ $\mu$ l and the primer sequences used to amplify the *Sp5*, *Wnt3*,  $\beta$ -catenin, *GFP* and *TBP* genes were designed with Primer3-OligoPerfect (ThermoFisher) (**Table S2**). Quantitative RT-PCR was performed using the SYBR Select Master Mix for CFX (Applied Biosystems) and a Biorad CFX96™ Real-Time System. Relative gene expression levels were calculated as described in [40], using *TBP* to normalize all data. Fold change (FC) values at each time point or condition were calculated over values obtained in non-electroporated animals. Finally at each condition, the FC values measured in  $\beta$ -catenin(RNAi) or *Sp5*(RNAi) animals were divided by those measured in animals of the same condition exposed to scramble dsRNA.

#### 2.7. Whole mount *In situ* hybridization (WM-ISH)

The animals were relaxed in 2% urethane/HM for 1 minute, and fixed in 4% PFA prepared in HM for 4 hours at room temperature (RT). The animals were washed several times with MeOH before being stored in MeOH at -20°C. WMISH was performed as described in [33]. For double WMISH, the *Wnt3* riboprobe was labeled with DIG (Sigma, Roche-11277073910) and the *Sp5* and *GFP* riboprobes labeled with fluorescein (Sigma, Roche-11685619910); the *Wnt3*-DIG riboprobe was co-incubated with either *Sp5*-FLUO or *GFP*-FLUO riboprobe during the hybridization step. At the development stage, the *Wnt3*-DIG riboprobe was first detected with NBT/BCIP (Sigma, Roche-11383213001) and the FLUO-labeled riboprobe subsequently detected with Fast Red. To stop NBT/BCIP reaction, samples were washed several times in NTMT, then incubated in glycine 100 mM, 0.1%Tween (pH 2.2) for 10 min and washed in Buffer I (1x MAB; 0.1% Tween). Next, samples were incubated in Buffer I supplemented with 10% sheep serum (Buffer I-SS) for 30

min at RT, prolonged for 1 hour with fresh Buffer I-SS at 4°C. Incubation with anti-FLUO-AP antibody (1:4000, Roche-1142638910) was done at 4°C overnight. The next day, samples were briefly washed in Buffer I then in 0.1M Tris/HCl (pH 8.2) 3x 10 min. Samples were developed with Fast Red (SigmaFAST, F4648). To stop the reaction, samples were washed several times in 0.1M Tris/HCl (pH 8.2) and fixed in 3.7% formaldehyde for 10 min at RT, rinsed in water and mounted in Mowiol. The co-detection of two riboprobes is technically challenging as NBT/BCIP detection of the DIG-labeled riboprobe, which is normally far more sensitive than the Fast Red detection of the fluorescein-labeled riboprobe, is much less efficient when tissues are treated for Fast Red. Consequently, we first analyzed the expression pattern of each gene separately, and subsequently co-detected *Wnt3* and *Sp5*, or *Wnt3* and *GFP* after ALP treatment. In these conditions, we found the co-detection highly informative to record context-specific regulations. The plasmids used to produce the riboprobes are listed in [Table S3](#).

### 2.8. Immunofluorescence

Animals were fixed and subsequently rehydrated as for WMISH with repeated washes in successive dilutions of EtOH in PBST (PBS, 0.5% Triton). Blocking was performed with 2% BSA in PBST for 1-2 hours at RT. For immunostaining, samples were incubated overnight at 4°C with an anti-GFP antibody (1:400, Novus NB600-308) in 2% BSA. Then, after several washes in PBST, the secondary antibody anti-rabbit coupled to Alexa 488 (1:600, Invitrogen A21206) was added in 2% BSA for 4 hours. For double immunofluorescence, the anti-mCherry (1:400, Abcam ab125096) and secondary anti-mouse coupled to Alexa 555 (1:600, Invitrogen A31570) antibodies were used.

### 2.9. Nuclear extracts (NEs) and Electro-Mobility Shift Assay (EMSA)

NEs were prepared according to [41]. Briefly, 100 *Hm-105* or *Hv\_AEP2* animals were washed rapidly in HM and once in Hypotonic Buffer (HB: 10 mM Hepes pH7.9, 2 mM MgCl<sub>2</sub>, 5 mM KCl, 0.5 mM spermidine, 0.15 mM spermine), then placed in a 1 ml glass douncer with 1ml HB and 20 strokes were given. After adding slowly (drop by drop) 210 µl of 2 M sucrose, 15 more strokes were given. The extract was centrifuged for 10 min at 3'200 rpm at 4°C, the pellet was washed twice with 800 µl Sucrose Buffer (0.3 M sucrose in HB) and resuspended in 50 µl Elution Buffer (glycerol 10%, 400 mM NaCl, 10 mM Hepes pH 7.9, 0.1 mM EDTA, 0.1 mM EGTA, 0.5 mM spermidine, 0.15 mM spermine) and incubated for 45 min. The eluate was centrifuged at 4°C for 20 min at 13'000 rpm, the supernatant aliquoted and stored at -80°C. All manipulations were carried out on ice and all buffers contain a mix of protease inhibitor cocktail (Bimake B14012).

The LightShift Chemiluminescent EMSA Kit (Thermo-Scientific, 89880) was used to perform EMSA with *Hydra* NE and biotinlabeled double-stranded oligos described in [Table S2](#). Briefly, 3 µl of *Hydra* NEs per 20 µl binding reaction were incubated for 20 minutes with the double-stranded oligos (20 fmol), then loaded on a 6% polyacrylamide gel (PAGE) in TBE 0.5x, electrophoresed and transferred onto a nylon membrane (BrightStar-Plus Invitrogen AM10102). Crosslink was done by exposing the membrane to UV-light 120 mJ/cm<sup>2</sup> for 30-50s (Marshall Scientific, SS-UV1800) and the samples fixed on the membrane were blocked for 15 minutes with Blocking Buffer (Thermo-Scientific 89880A). The membrane was conjugated with Stabilized Streptavidin-Horseradish Peroxidase (1:300, Thermo-Scientific, 89880D), developed by adding Luminol/Enhancer solution (Thermo-Scientific 89880E/F).

### 2.10. Production of anti-*Sp5* antibodies

Two anti-*Sp5* antibodies were generated. A rabbit polyclonal antibody was produced by Covalab (Bron, France) against three peptides P1 (178-191): NEHHIKEYSEHSQA, P2 (398-411): CDENVMELEVNVEN and P3 (155-175): PASPISWLFPQNIIQSHPSKV. After four immunizations the sera were collected from a single rabbit and ELISA test was performed to check immunoreactivity. Next the sera were purified by Covalab with the peptides P1 and P2 to remove any P3 cross-reactivity. The mouse monoclonal antibody was produced by Proteogenix (Schiltigheim, France) against a 6His-tag (MGSHHHHHHS) 251  
252  
253  
254  
255  
256

coupled to a 218 AA-long *Hydra* Sp5 fragment (ISPLEQT---YSMSTSI) produced chemically. The Sp5-218 protein (24.5 kDa) was expressed in *E. coli* and injected to the animals. After four immunizations, spleen cells collected from two mice were fused to myeloma cells. The antibody, produced from one selected clone, was validated by IP analysis.

### 2.11. Cell culture and whole cell extracts (WCEs) and Western blotting

HEK293T cells were cultured in DMEM High Glucose, 10% fetal bovine serum (FBS), 6 mM L-glutamine, and 1 mM NA pyruvate in 10 cm diameter cell culture dishes (CellStar, Greiner Bio-One 664160). After a two-day growth, the cells were collected by scraping, counted and  $15 \times 10^4$  cells per well were seeded in 6-well plates and grown for 19 hours. Next, cells were transfected with 2  $\mu$ g of pCS2+empty or pCS2+*HySp5* plasmid using the X-tremeGENE HP DNA transfection reagent (Sigma, 6366546001). To prepare cell extracts 24 hours later, cells were resuspended in PBS 1x before being centrifuged for 3 min at 3'000 rpm at 4°C. After discarding the supernatant, the pellet was resuspended in fresh Lysis Buffer (LB): 50 mM Hepes pH 7.6, 150 mM NaCl, 2.5 mM MgCl<sub>2</sub>, 0.5 mM DTT, 10% glycerol, 1% Triton 100x, 0.1 mg/ml PMSF, 10% protease inhibitor cocktail (Bimake, B14012) and a lab-made phosphatase inhibitors cocktail (8 mM NaF, 20 mM  $\beta$ -glycerophosphate, 10 mM Na<sub>3</sub>VO<sub>4</sub>). After a 30 min incubation on ice, the extract was centrifuged at 14'000 rpm for 10 min at 4°C, the supernatant was aliquoted and stored at -80°C.

20  $\mu$ g extracts, either WCEs or NEs, were diluted with Loading Laemmli buffer and then boiled for 5 minutes at 95°C before being loaded onto a 10% SDS-PAGE, then electrophoresed and transferred onto a PVDF membrane (Bio-Rad 162-0177). Next, the membrane was blocked for 1 hour at RT with 5% dry milk in TBS 1x, 0.1% Tween (TBS-T). Anti-Sp5 antibodies were added at a 1:500 dilution and incubated overnight at 4°C. The membranes were washed 3x 10 minutes in TBS-T before being incubated for 2 hours with the secondary anti-mouse-HRP- or anti-rabbit HRP antibody (1:5000, Promega anti-mouse, W4021; anti-rabbit W4011). The membranes were washed in TBS-T for 3x 10 minutes and developed with Western Lightning Plus-ECL reagent (Perkin Elmer NEL104). To produce *in vitro* the Sp5 protein, the pCS2+empty and pCS2\**HySp5* plasmids were incubated using the TNT Quick Coupled Transcription/Translation Systems (Promega L2080) and 1  $\mu$ l was loaded on 10% SDS-PAGE.

### 2.12. Chromatin Immuno-precipitation and quantitative PCR (ChIP-qPCR)

ChIP was performed with 300 *Hm105* or *Hv\_AEP2* animals fixed in 1% Formaldehyde Solution (Thermo-Scientific 28906) for 15 min, then transferred in Stop Solution (Active Motif 103922) for 3 min, briefly washed in cold HM before being resuspended in 5 ml Chromatin prep buffer containing 0.1 mM PMSF, 0.1% protease inhibitor cocktail (Active Motif 103923). Samples were transferred to pre-cooled 15 ml glass douncers and crushed with 30 strokes. The samples were incubated on ice for 10 minutes before being centrifuged at 4°C for 5 min at 1'250 rcf. Each pellet was resuspended in 1 ml Sonication Buffer (SB: 1% SDS, 50 mM Tris-HCl pH 8.0, 10 mM EDTA pH 8.0, 1 mM PMSF, 1% protease inhibitor cocktail) and incubated on ice for 10 minutes. The chromatin was then sonicated with a Diagenode Bioruptor Cooler (sonication conditions: Amp: 25%, Time: 20s on, 30s off, 2 cycles). The samples were centrifuged at 14'000 rpm for 10 minutes at 4°C, the supernatant was sonicated (sonication conditions as above but 3 cycles), centrifuged at 14'000 rpm for 10 minutes at 4°C, and the supernatant recovered. After measuring DNA with Qubit, 10  $\mu$ g of the sonicated chromatin were diluted (1:5) in ChIP Dilution Buffer (DB: 0.1% NP-40, 0.02 M Hepes pH 7.3, 1 mM EDTA pH 8.0, 0.15 M NaCl, 1 mM PMSF, 1% protease inhibitor cocktail) and incubated with 1  $\mu$ g of either monoclonal or polyclonal  $\alpha$ -Sp5 antibody or pre-immune serum antibody overnight at 4°C on a rotating wheel. The sample was then loaded onto a ChIP-IT ProteinG Agarose Column (Active Motif 53039), incubated on a rotating wheel for 3 hours at 4°C, washed 6 times with 1 ml Buffer AM1 before being eluted with 180  $\mu$ l Buffer AM4. After, 1M NaCl and 3x TE buffer were added to perform decrosslinking overnight at 65°C. Next, RNase A (10  $\mu$ g/ $\mu$ l) was added for 30 min at 37°C followed by Proteinase K (10  $\mu$ g/ $\mu$ l) for 2 hours at 55°C. Finally, the MiniElute

PCR purification kit (Qiagen, 28004) was used to purify the samples. DNA was eluted in 30  $\mu$ l and 1  $\mu$ l per condition was used for qPCR.

### 2.13. Imaging

Live imaging to analyze the dynamics of mCherry and GFP fluorescence was performed on the Leica DM5500 microscope using the Leica software. To quantify GFP fluorescence, the acquired data were analyzed with Fiji (ImageJ). The same microscope was used to image immunofluorescence on whole animals. A confocal LSM780 microscope was used to image with high magnification the immunostained hypostome region of transgenic animals, as well as the budding region of live transgenic animals. In this latter case, animals were incubated in 1 mM linalool in HM for 10 min prior to imaging, then kept in the linalool solution between two coverslips separated by a 0.025 mm spacer. WMISH pictures were acquired with the Olympus SZX10 microscope.

### 2.14. Statistical analyses

The statistical analyses were two-tailed unpaired and were carried out using the GraphPad Prism software. P values are for  $**** \leq 0.0001$ ,  $*** > 0.0001$  and  $\leq 0.001$ ,  $** > 0.001$  and  $\leq 0.01$ ,  $* > 0.01$  and  $< 0.05$ ,  $ns \geq 0.05$ .

## 3. Results

### 3.1. Differential *Sp5* regulation in the epidermal and gastrodermal layers along the body axis

To monitor the regulation of *Sp5* expression in the epidermal and gastrodermal epithelial layers, we produced a tandem reporter construct *HyAct-1388:mCherry\_HySp5-3169:GFP* where the *Hydra Actin* promoter (*HyAct*, 1388 bp) drives the ubiquitous expression of mCherry and the *Hydra Sp5* promoter (*HySp5*, 3169 bp) drives eGFP expression (**Figure 1B**, **Figure S2**). After injecting the reporter construct into *Hv\_AEP2* embryos, two transgenic lines were obtained by clonal amplification, one expressing the reporter in the epidermis (epidermal\_*HySp5-3169:GFP*) and the other in the gastrodermis (gastrodermal\_*HySp5-3169:GFP*). Next, we compared in q-PCR analysis the expression levels of *Sp5*, *GFP* and *Wnt3* in the apical, central body column and basal regions of each transgenic line (**Figure 1C**, **1D**). As expected, we found in both lines *Wnt3* expressed exclusively apically and *Sp5* expressed in all regions but at maximal levels apically. By contrast, *GFP* appears differentially regulated along the body axis between the two lines, with an apical-to-basal graded expression in epidermal\_*HySp5-3169:GFP* animals, and a similar high level of expression in the apical region and the upper half of the body column in gastrodermal\_*HySp5-3169:GFP* animals, followed by a low expression in the basal region (**Figure 1C**, **1D**). These results indicate that the *Sp5-3169* promoter is differentially regulated along the body column in the epidermal and gastrodermal layers.

This result was confirmed at the protein level by recording live fluorescent GFP (**Figure 1E,1F**) or by immunodetecting GFP (**Figure 1G,1H**). In epidermal\_*HySp5-3169:GFP* animals, GFP fluorescence and GFP protein are detected in the epidermal layer over the whole hypostome, the tentacle ring, the proximal part of the tentacles and the upper body column (**Figure 1E,1G**, **Figure S3A,S3C**). In gastrodermal\_*HySp5-3169:GFP* animals, GFP fluorescence and GFP protein extends over a broad domain in the gastrodermal layer, from the apical region throughout the body column (**Figure 1F,1H**, **Figure S3B,S3D**). However, the tip of the hypostome is free of gastrodermal GFP fluorescence and GFP protein (see enlarged head in **Figure 1F**, arrows in **Figure 1H**), an area where *Wnt3* expression is maximal and endogenous *Sp5* expression minimal [27,33].

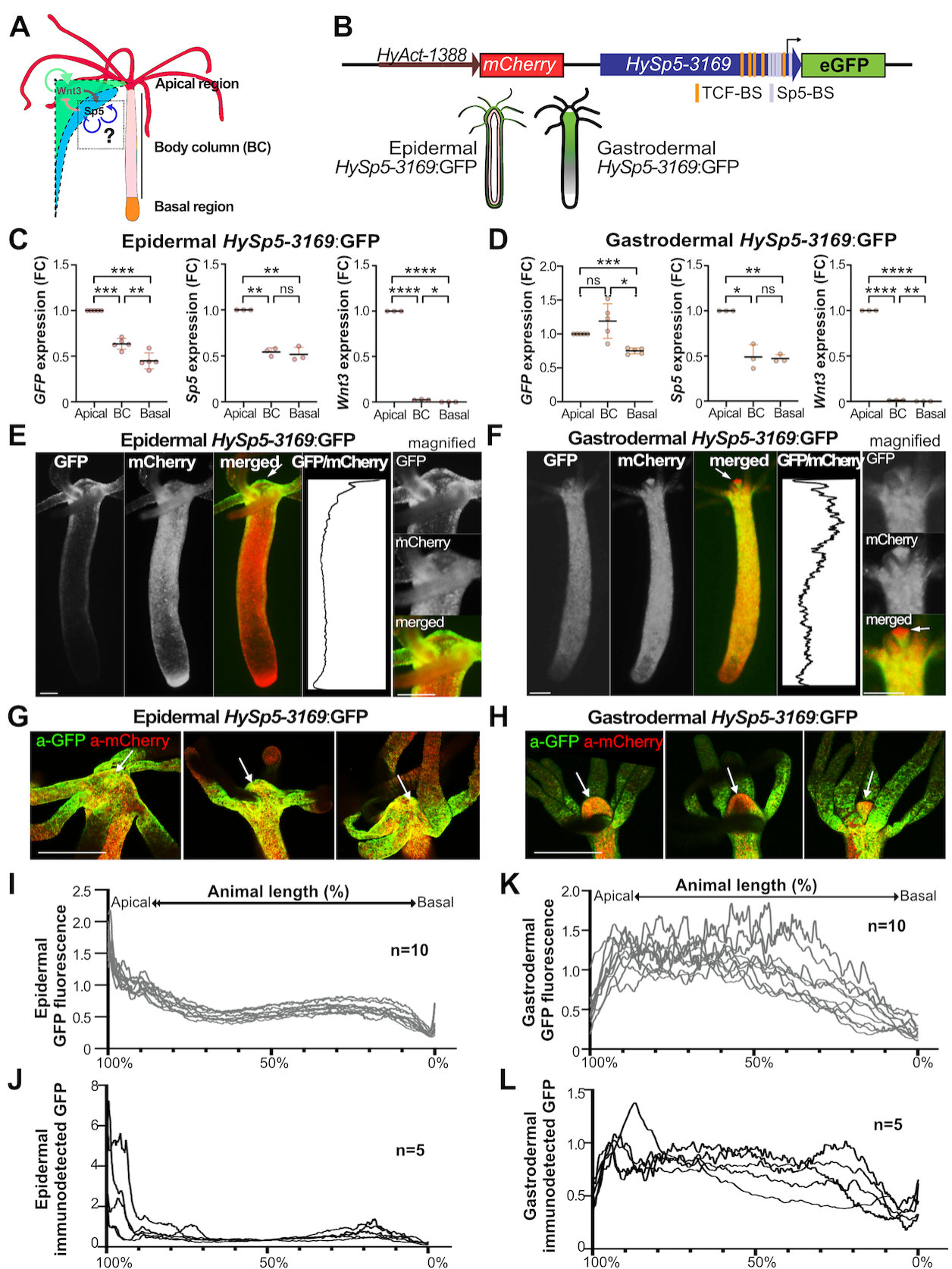


**Figure 1. Differential regulation of *HySp5-3169:GFP* expression in the epidermal and gastrodermal layers.** (A) *Hydra* anatomy includes the apical region or head, formed of a dome-shape named hypostome, centered around the oral opening, surrounded by a ring of tentacles at its basis, the elongated body column and the basal disc or foot that can attach to substrates. The scheme on the left shows the *Wnt3* (green) and *Sp5* (blue) expression profiles along the body axis together with the positive and negative interactions between *Wnt3* and *Sp5*, and the putative *Sp5* auto-regulation in

Hydra (Vogg et al., 2019). **(B)** Structure of the *HyAct-1388:mCherry\_HySp5-3169:GFP* reporter construct used to generate two transgenic lines, epidermal *HySp5-3169:GFP* and gastrodermal *HySp5-3169:GFP*, where epithelial cells from the epidermis and the gastrodermis respectively express GFP and mCherry (see [Figure S2](#)). TCF-BS: TCF-binding sites (orange); Sp5-BS: Sp5-binding sites (grey). **(C, D)** Q-PCR analysis of *GFP*, *Sp5* and *Wnt3* expression in the apical, body column (BC) and basal regions of epidermal *HySp5-3169:GFP* (C) and gastrodermal *HySp5-3169:GFP* (D) animals fixed immediately after dissection. P values: \*\*\* $\leq$  0.0001, \*\* $\leq$  0.001, \* $\leq$  0.01, ns  $\geq$  0.05. **(E, F)** Live imaging of *HySp5-3169:GFP* animals with eGFP (green), mCherry (red); the apical region of each animal is magnified on the right. White arrows point to the tip of the hypostome. The graphs show the eGFP/mCherry fluorescence intensity ratios (Relative eGFP intensity) along the animal axis. **(G, H)** Immunodetection of GFP (green) and mCherry (red) in the apical region (white arrow) of epidermal *HySp5-3169:GFP* (G) and gastrodermal *HySp5-3169:GFP* (H) animals. **(I-L)** Graphs showing the relative GFP fluorescence recorded live (I, K) or after immunodetection (J, L) measured in epidermal (I, J) or gastrodermal (K, L) *HySp5-3169:GFP* animals. The apical extremity is on the left (100%), the basal one on the right (0%). Scale bar: 250  $\mu$ m. See [Figure S3](#).

These analyses show that 3169 bp sequences of the *Sp5* promoter are sufficient to recapitulate the previously identified endogenous *Sp5* expression pattern in the apical region and along the body column [33] and to highlight previously unrecognized differences in expression between epidermis and gastrodermis.

From the GFP and mCherry fluorescence profiles, we produced a relative GFP intensity profile for each animal that corresponds to the GFP/mCherry ratio at all points along the body axis ([Figure 1I, 1K](#), [Figure S3E, S3F](#)). By grouping the profiles of 10 animals, we concluded that live epidermal GFP fluorescence is graded apical-to-basal, from 100% to 70% body length, then maintained at low levels between positions 70% to 10% ([Figure 1I](#), [Figure S3E](#)). By contrast, in live gastrodermal *HySp5-3169:GFP* animals the GFP levels are low at the tip (position 100%-90%), reach a high plateau value from position 90% up to 40% body-length, and then decline towards the basal extremity ([Figure 1K](#), [Figure S3F](#)). For each transgenic line, the GFP fluorescence intensity profiles in live animals match the profile of immunodetected GFP in corresponding fixed samples ([Figure 1J, 1L](#)). Therefore, the comparative analysis of *GFP* transcripts, GFP fluorescence and GFP protein converge to identify distinct patterns in the epidermis and gastrodermis, both apically and along the body axis, indicating that *Sp5* is differentially regulated in these two layers.

### 3.2. *Sp5* regulation after bisection is systemic in gastrodermis but localized in epidermis

Next, we analysed how *HySp5-3169:GFP* is regulated in developmental contexts. In epidermal *HySp5-3169:GFP* animals bisected at mid-gastric level, we noted a low or none *GFP* expression in apical-regenerating (AR) tips fixed at 8 and 12 hours post-amputation (hpa), later on detected at 24 hpa ([Figure 2A](#), [Figure S4A](#)). At 48 hpa, tentacle rudiments that emerge do not express *GFP* whereas the tip of the developing hypostome strongly expresses *GFP*; at 72 hpa, the epidermal *GFP* pattern is typical, with maximal expression at the root of tentacles. By contrast, in gastrodermal *HySp5-3169:GFP* animals, *GFP* is detected immediately after bisection, possibly artefactual in the injured tissues, then at high levels in a broad domain encompassing the AR tips at 8, 12 and 24 hpa ([Figure 2B](#), [Figure S4B](#)). At 48 hpa, the gastrodermal apical *GFP* expression becomes restricted, leaving the emerging tentacles and the tip of the future hypostome free of expression. At 72 hpa, apical *GFP* expression is mostly at the level of the tentacle ring, absent from tentacles and hypostome, with some low level of expression in the peduncle region. Along the body column of regenerating animals, we also identified two distinct patterns of gastrodermal *GFP* expression, either high levels in stripes, or diffuse throughout the animal.

During basal regeneration, *GFP* expression is excluded from the basal-regenerating (BR) half in epidermal *HySp5-3169:GFP* animals at all time-points ([Figure 2A](#), [Figure S4C](#)). At 48 hpa, most animals have differentiated a new basal disc and *GFP* expression is slightly up-regulated in the peduncle region. In gastrodermal *HySp5-3169:GFP* animals, the immediate *GFP* signals observed in the BR tips might be artefactual, linked to injury as in AR tips ([Figure 2B](#), [Figure S4D](#)). At subsequent stages, *GFP* expression is quite

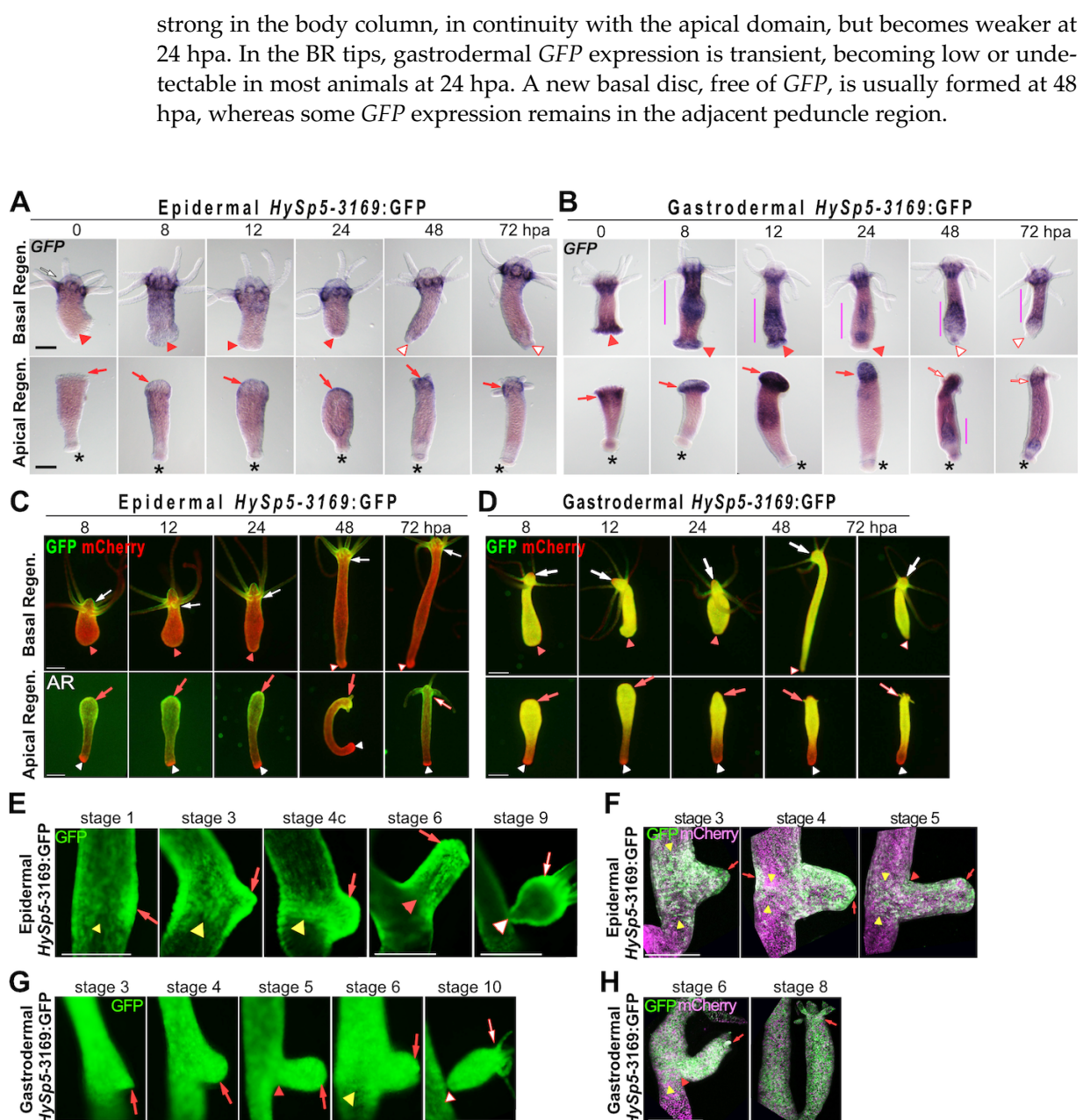


**Figure 2. GFP regulation in regenerating and budding *HySp5-3169:GFP* transgenic animals.**

(A, B) GFP expression in regenerating halves from epidermal (A) and gastrodermal (B) *HySp5-3169:GFP* transgenic animals bisected at t0 and fixed at indicated times. Regen.: regeneration; hpa: hours post-amputation; red arrows point to apical-regenerating (AR) regions, red triangles to the basal-regenerating (BR) regions; vertical bars indicate gastrodermal GFP expression along the body column, asterisks the original basal discs, white triangles outlined red to the regenerated basal discs. See [Figure S4](#). (C, D) GFP (green) and mCherry (red) fluorescences in AR and BR halves of *HySp5-3169:GFP* transgenic animals pictured live at indicated time points. White arrows point to apical regions of original polyps, red arrows to AR regions, white arrows outlined red to regenerated heads; white arrowheads to original mature basal discs, red arrowheads to the BR regions. See [Figure S5](#). (E-H) Live imaging of budding *HySp5-3169:GFP* transgenic animals, either epidermal (E) or gastrodermal (F), pictured at indicated stages with the Olympus SZX10 microscope (E, G, GFP fluorescence only), or the Zeiss LSM780 microscope (F, H, GFP and mCherry fluorescence). On the parental polyp, yellow arrowheads point to the “budding belt” that forms in the budding zone; on the developing buds, red arrows point to the developing apical region, red arrowheads to the differentiating basal region and white arrowheads to fully differentiated basal discs. Scale bar: 250  $\mu$ m.

423  
424  
425  
426  
427  
428  
429  
430  
431  
432  
433  
434  
435  
436  
437  
438

At the protein level, GFP fluorescence can be detected during apical regeneration at high level in both layers at 8, 12 and 24 hpa, with a similar broad pattern extending along the AR half, leaving free the peduncle region (**Figure 2C,2D**, **Figure S5**). Subsequently, when tentacle rudiments appear, the epidermal GFP fluorescence becomes maximal in the apical region and graded along the body column, while the gastrodermal one vanishes from the tip of the forming head while becoming predominant in the tentacle ring and upper body column, like the homeostatic pattern. As expected, no GFP fluorescence is observed in the epidermal\_ *HySp5-3169*:GFP halves regenerating their basal half, except in the original apical region (**Figure 2C**, **Figure S5A**); in gastrodermal\_ *HySp5-3169*:GFP animals, the GFP fluorescence is broadly distributed along the body axis, becoming excluded from the differentiating basal disc as observed at 48 hpa (**Figure 2D**, **Figure S5B**).

During budding, GFP fluorescence is detected throughout the whole process in both the epidermal and gastrodermal layers of *HySp5-3169*:GFP animals although with different features (**Figure 2E-2H**). In the parental polyp, GFP fluorescence in the epidermis is first visible as a patch preceding morphological detection of the bud (stage 1, **Figure 2E**), then in the budding belt where the GFP domain progressively forms well-defined boundaries, persisting until stage 6 of budding (**Figure 2E,2F**). In the gastrodermis, GFP fluorescence is also detected in the budding belt, but with rather diffuse boundaries, in continuity on the apical side with the GFP expression domain along the body column (**Figure 2G,2H**). In the growing bud, GFP fluorescence is ubiquitously expressed in both layers, becoming predominantly apical in the epidermal layer from stage 6 onwards. At stages 9 and 10, the bud is mature and ready to detach. The spatial patterns of epidermal and gastrodermal GFP fluorescence correspond to those observed in adult polyps, apically restricted in the epidermis, while diffuse along the axis in the gastrodermis (**Figure 2E,2G**).

In summary, the epidermal and gastrodermal *HySp5-3169*:GFP transgenic lines provide the means to visualize the temporal and spatial layer-specific regulations of *Sp5* linked to regeneration and budding. During apical regeneration, *Sp5* is up-regulated in the epidermis at an early-late phase (24 hpa), and not at all during basal regeneration. In contrast, gastrodermal GFP expression is broadly enhanced at an early stage along the regenerating halves, regardless of the type of regeneration, apical or basal. This generalized increase in gastrodermal GFP expression reflects a systemic *Sp5* response to amputation, specifically driven by the *Sp5* promoter as such increase was not observed with *mCherry* driven by the *Actin* promoter. Moreover, the analysis of the budding process shows a tightly regulated expression of *Sp5* in the epidermis, versus a rather diffuse and systemic one in the gastrodermis.

### 3.3. Layer-specific modulations of *Sp5* expression upon alsterpaullone (ALP) treatment

We then compared the phenotypic changes induced by the GSK3 $\beta$  inhibitor Alsterpaullone (ALP), which in the *H. vulgaris* Zürich L2 strain (*Hv\_ZüL2*) leads to an increase in the level of nuclear  $\beta$ -catenin in the body column and subsequent activation of Wnt3/ $\beta$ -catenin signaling [23] (**Figure 3A**). As a result, a two-day ALP treatment induces the formation of multiple ectopic tentacles along the body column of *Hv\_ZüL2* or *Hv\_Basel* animals [23,33]. However, in animals from the *Hv\_AEP2* strain, a two-, four- or even seven-day ALP treatment only leads to the transient and partial development of few ectopic tentacles along the body column, likely as a result of the lower sensitivity of *Hv\_AEP2* animals to drug treatments [42].

Nevertheless, after a four-day treatment, we noticed additional morphogenetic changes such as the striking reduction in size of both the original tentacles and the hypostome at the apical pole, together with the enlargement of the upper body column that appears globally “swollen”, and the progressive disappearance of the basal disc and the refinement of the basal extremity (**Figure 3B**, **Figures S6-S8**). Given the positive feedback loop that operates between Wnt3/ $\beta$ -catenin, *Sp5* and *Zic4*, and the negative one between *Sp5* and *Wnt3*, we investigated how *Sp5* expression is modulated in each epithelial layer

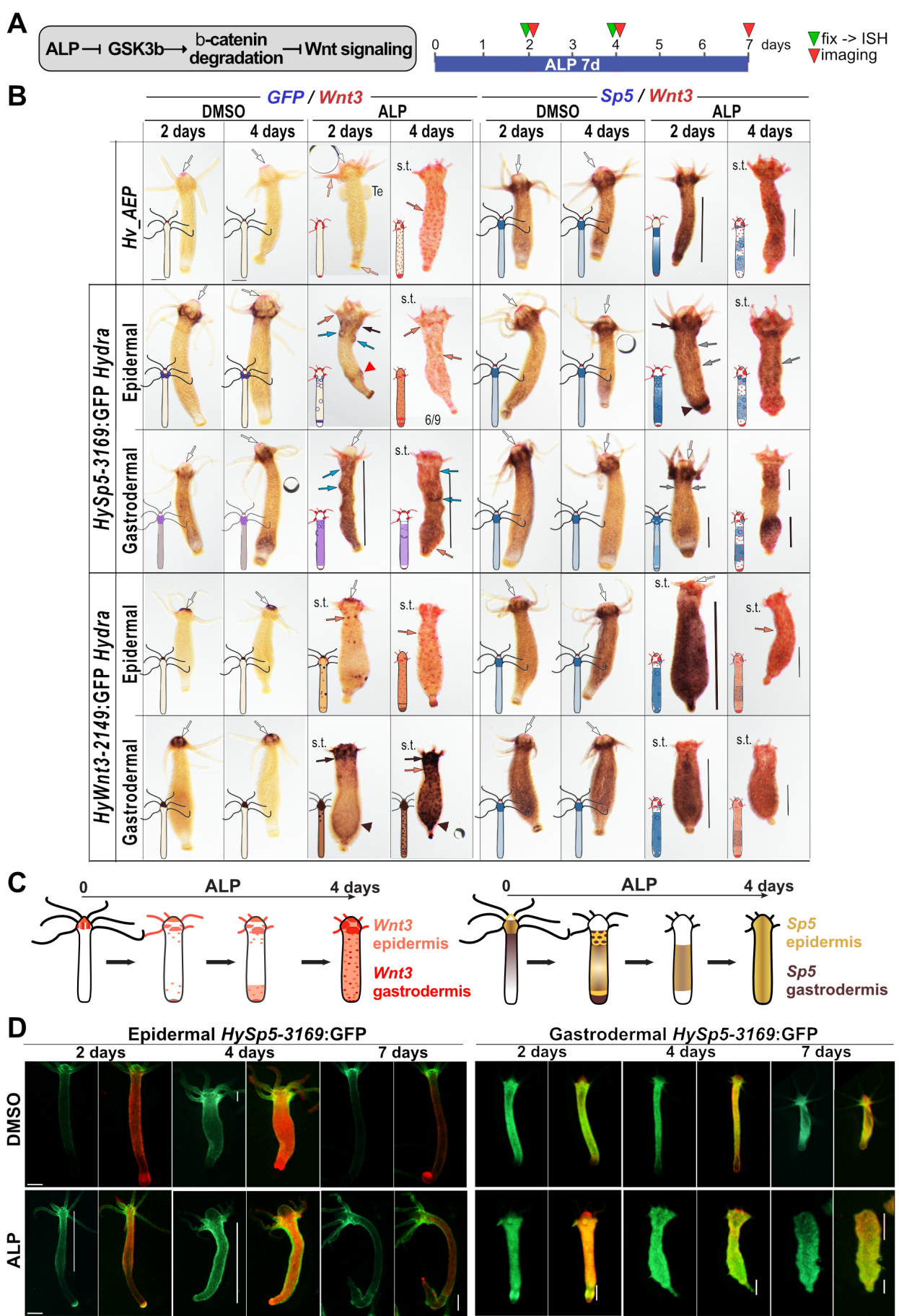


**Figure 3. Alsterpaullone-induced modulations of GFP, Wnt3 and Sp5 expression along the epidermis and gastrodermis of *HySp5-3169:GFP* and *HyWnt3-2149:GFP* transgenic Hydra.**

(A) Schematic representation of the activating effect of ALP on Wnt/β-catenin signaling. (B) Co-detection of GFP and Wnt3 (left half), or Sp5 and Wnt3 (right half) in wild-type (*Hv\_AEP*) animals or in transgenic animals that constitutively express the *HySp5-3169:GFP* or *HyWnt3-2149:GFP* constructs, after a 2- or 4-day ALP exposure. Black arrows: expression immediately below the apical region; black arrowheads: ALP-induced GFP expression in the peduncle zone; grey arrows: ALP-induced circular zones of Sp5 expression along the body column; orange arrows: Wnt3-expressing spots along the body column; white arrows: Wnt3 expression at the tip of the hypostome; vertical black bars: areas of ALP-induced GFP expression along the body column; s.t.: short tentacles. (C) Schematic representation of the ALP-induced modulations of Wnt3 and Sp5 in the epidermal and gastrodermal *HySp5-3169:GFP* and *HyWnt3-2149:GFP* transgenic lines. See **Figures S6, S7, S8**. (D) Live imaging of mCherry and GFP fluorescence in epidermal and gastrodermal *HySp5-3169:GFP* animals treated for 2, 4 and 7 days with ALP or DMSO. For each condition, GFP fluorescence is shown on the left, and the merged GFP (green) and mCherry (red) fluorescence on the right. Vertical white bars indicate areas of ectopic GFP fluorescence. Scale bar: 250 μm.

when β-catenin signaling is constitutively activated. We thus exposed non-transgenic and *HySp5-3169:GFP* transgenic animals to ALP for two or four days and analyzed the concomitant modulations of Sp5 and Wnt3, and of GFP and Wnt3 (**Figure 3B**, **Figures S6, S7**).

After two days, we observed in all conditions a transient extension of the apical Sp5 and *HySp5-3169:GFP* expression domain (i.e. positive for both Sp5 and GFP) below the head, forming a second tentacle ring, from which, in some animals, ectopic tentacles transiently emerge. In the body column, Sp5 is globally up-regulated along the gastrodermis while about half of the epidermal *HySp5-3169:GFP* animals form circular figures along the upper body column, possibly outlining regions where ectopic structures are transiently induced (**Figure 3B**, **Figure S7**). We also noted in both epidermal and gastrodermal *HySp5-3169:GFP* animals, a high level of GFP expression close to the basal extremity, including a GFP+ ring just above the basal disc.

After four days, most of the two-day ALP-induced changes have vanished: Sp5 and GFP are no longer detected apically, neither in the epidermis, nor in the gastrodermis, the Sp5/GFP epidermal figures along the body column have disappeared, and the global epidermal GFP expression is dramatically reduced. In the gastrodermis, the *HySp5-3169:GFP* expression remains present in the central part of the body column in most animals (**Figure 3B**, **Figure S7**). In summary, this analysis shows a similar silencing of epidermal and gastrodermal *HySp5-3169:GFP* in the apical region, but striking differences along the body column, with *HySp5-3169:GFP* transiently enhanced and forming circular figures in the epidermis, while remaining diffuse and long-lasting in the gastrodermis.

**3.4. Layer-specific modulations of Wnt3 expression induced by ALP treatment**

In parallel, we tested the putative layer-specific modulations of Wnt3 by exposing to ALP animals of the epidermal and gastrodermal *HyAct-1388:mCherry\_HyWnt3-2149:GFP* transgenic lines (named *HyWnt3-2149:GFP*) where GFP expression is under the control of 2'149 bp of the Wnt3 promoter [27,33] (**Figure S8**). Regarding Wnt3 regulation after a two-day ALP treatment, the epidermal *HyWnt3-2149:GFP* persists at the tip of the hypostome while strongly up-regulated in the tentacle area and in tentacle roots, and few small dots expressing Wnt3 and *HyWnt3-2149:GFP* become visible along the body column. After a four-day ALP treatment, as expected, Sp5 is strongly down-regulated, while a dense network of Wnt3 or *HyWnt3-2149:GFP* dots is established along the entire body column in both layers (**Figure 3B**, **Figure S6-S8**). We also noted a strong overall increase in gastrodermal *HyWnt3-2149:GFP* expression along the body column, indicating that the transactivation driven by the *HyWnt3-2149* promoter in the gastrodermis is much greater than that driven by the full set of regulatory sequences of the endogenous *HyWnt3* gene.

In summary, the analysis of epidermal and gastrodermal GFP expression in these four transgenic lines help identify layer-specific regulations of Sp5 and Wnt3 in response

to the ALP-induced activation of Wnt/β-catenin signaling (Figure 3C). The monitoring of GFP fluorescence in *HySp5-3169*:GFP animals confirmed these layer-specific differences, i.e. a transient *Sp5* up-regulation in the body column after two or four days of ALP exposure, followed by a down-regulation when Wnt3/β-catenin signaling is highly active, mimicking the situation at the tip of the hypostome. Indeed, after a seven-day ALP treatment, *HySp5-3169*:GFP fluorescence is restricted to the modified apical and basal extremities in epidermal transgenic animals, and shifted to the lower half of the body in gastrodermal ones (Figure 3D).

### 3.5. β-catenin knock-down differentially impacts *Sp5* expression in epidermis and gastrodermis

To test a possible layer-specific regulation of *Sp5* when β-catenin signaling is reduced, we knocked-down β-catenin in *HySp5-3169*:GFP transgenic animals (Figure 4A). As early as 24 hours after the 1st electroporation (EP), we found the normalized levels of β-catenin transcripts significantly decreased, by about 2-fold in the epidermis and gastrodermis of the apical region, and by 2-fold along the gastrodermis of the body column. Paradoxically, in *HySp5-3169*:GFP gastrodermal animals exposed to non-specific scrambled siRNAs, the β-catenin transcript levels increase steadily after each EP in both apical and body column regions. This observation suggests that the EP procedure leads to an unspecific stress-induced response that either activates β-catenin regulatory sequences, and/or stabilizes β-catenin transcripts (Figure 4B, Figure S9).

With regard to *Sp5* levels, we did not detect any specific modulation, with the exception of a transient decrease one day post-EP2 along the body column of gastrodermal *HySp5-3169*:GFP animals (Figure 4B, Figure S9). Concerning the GFP levels, we recorded in the apical and body column regions of the epidermal *HySp5-3169*:GFP animals a progressive decrease, below 25% in the apical region one day after EP3, a result that likely reflects a weaker activation of the *HySp5-3169* promoter in the epidermis when β-catenin expression is decreased. We also noted in animals exposed to scrambled siRNAs a twofold increase in the level of epidermal GFP transcripts along the body column, again pointing to an EP-induced stress response. The consequences of β-catenin knock-down are different in the gastrodermis, actually quite limited with a transient increase in the *HySp5-3169*:GFP transcript level in the apical region one day after EP2 without any significant modulation in the body column. It should be noted that the non-specific EP-induced increase in GFP observed in the epidermis is not observed in the gastrodermis.

In summary, the β-catenin RNAi procedure efficiently reduces the level of β-catenin transcripts, up to twofold in both the epidermis (mainly apical) and the gastrodermis (apical and body column). This β-catenin reduction does not affect the levels of *Sp5* transcripts outside the -1.41 / + 1.41 fold range (except at one time-point in the gastrodermal body column). Notably it strongly affects the *HySp5-3169*:GFP transcript levels in the epidermis where a two to four-fold reduction (apical and body column) is noted. Such an effect is not observed in the gastrodermis. Finally, we noted that the RNAi procedure produces an EP-induced stress response in the body column leading to an unspecific increase in β-catenin levels in the gastrodermis and in *HySp5-3169*:GFP levels in the epidermis.

### 3.6. β-catenin knock-down leads to formation of pseudo-buds that express gastrodermal *Sp5*

We previously showed that a transient knock-down of β-catenin triggers a size reduction in *Hv\_Basel* animals, as well as the formation of “pseudo-buds”, defined as lateral structures that grow from the body column similarly to buds but without forming a complete head with a fully differentiated ring of tentacles [33]. These pseudo-buds are present in 100% of *Hv\_Basel* animals one day after EP3 (Figure S10). Remarkably, as early as two days after EP1, well-defined regions along the parental polyp are already strongly expressing *Sp5*, even before pseudo-buds become morphologically visible (Figure 4C, Figure S10).

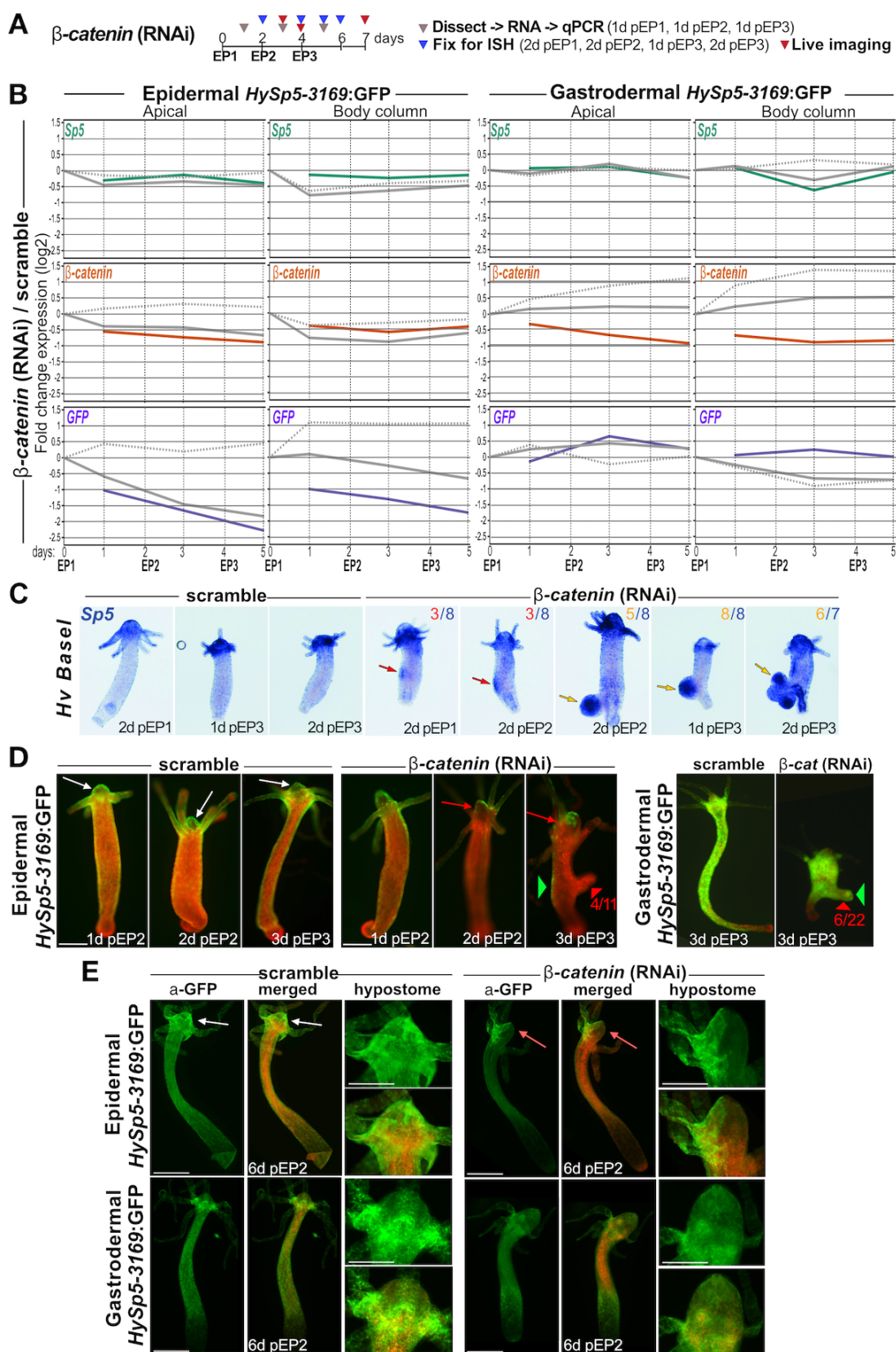


**Figure 4. Impact of  $\beta$ -catenin(RNAi) on *Sp5* expression in *Hv-Basel* and *HySp5-3169:GFP* transgenic animals. (A)** Schematic view of the procedure: After one, two or three electroporations (EP1, EP2, EP3) with scramble or  $\beta$ -catenin siRNAs, animals were either dissected in apical and body column regions for RNA extraction (grey triangles) or fixed for whole mount in situ hybridization (ISH, blue triangles), or imaged live (red triangles) at indicated time-points (d pEP: day(s) post-EP). **(B)** Q-PCR analysis of *Sp5*,  $\beta$ -catenin and *GFP* transcript levels in apical (100%-80%, left) and body column (80%-0%, right) regions of epidermal (left) and gastrodermal (right) *HySp5-3169:GFP*

595  
597  
598  
599  
600  
601

transgenic animals taken one or two days after EP1 (days 1, 2), after EP2 (days 3, 4), or one day after EP3 (day 5). In each panel, the colored line corresponds to the Fold Change (FC) values between  $\beta$ -catenin RNAi animals (continuous grey lines) and control animals exposed to scramble siRNAs (dotted grey lines), which are each expressed as FC relative to non-electroporated animals at time 0, just before EP1. See **Figure S9**. (C) *Sp5* expression pattern and phenotypic changes in scramble and  $\beta$ -catenin (RNAi) *Hv\_Basel* animals at indicated time-points. Red arrows point to *Sp5*-expressing patches along the body column, yellow arrows to pseudo-bud structures that express *Sp5* and become multiple two days pEP3 without differentiating apical structures. See **Figure S10**. (D) GFP (green) and mCherry (red) fluorescence in  $\beta$ -catenin (RNAi) *HySp5-3169*:GFP transgenic live animals. GFP fluorescence in apical regions is either normal (white arrows) or missing (red arrowheads). Note the transient pseudo-bud structures that develop after  $\beta$ -catenin (RNAi) (red arrowheads) and express GFP in gastrodermal *HySp5-3169*:GFP animals (green triangles). See **Figure S11**. (E) Immunodetection of GFP and mCherry in *HySp5-3169*:GFP animals 6 days post-EP2 (6d pEP2). Apical regions of scramble and  $\beta$ -catenin (RNAi) animals are magnified on the right. White and red arrows as in D. See **Figure S12**. Scale bar: 250  $\mu$ m.

Concerning GFP and mCherry fluorescence in epidermal *HySp5-3169*:GFP animals, the control animals exposed to scramble siRNAs show the expected pattern of high-level GFP fluorescence in the apical region and a low one along the body column. Meanwhile the  $\beta$ -catenin (RNAi) animals exhibit two days post-EP2 a loss of GFP fluorescence in well-defined areas of the apical region together with a globally reduced GFP fluorescence along the body column except for some GFP-positive patches (**Figure 4D**, **Figure S11A**). Three days post-EP3, newly formed pseudo-bud structures become visible in 30% to 60% of the animals, and those never show any epidermal GFP fluorescence. We confirmed these findings by immuno-detecting GFP and mCherry in epidermal *HySp5-3169*:GFP animals knocked-down for  $\beta$ -catenin.

We noted the loss of epidermal GFP expression in large parts of the apical region, the presence of GFP-positive patches along the body column and the lack of GFP protein in the pseudo-bud structures (**Figure 4E**, **Figure S12**). In gastrodermal *HySp5-3169*:GFP animals knocked-down for  $\beta$ -catenin, the gastrodermal layer remains GFP fluorescent in the tentacle ring and along the body column. The pseudo-buds are all GFP fluorescent, with positive signal in the presumptive apical region and often with a patchy pattern (**Figure 4D**, **Figure S11B**). We could confirm these findings by immunodetecting GFP and mCherry six days post-EP2 in these animals (**Figure 4E**, **Figure S12**).

In summary,  $\beta$ -catenin(RNAi) leads to the formation of pseudo-bud structures in both *Hv\_Basel* and *Hv\_AEP2* animals, a phenotype observed with a higher penetrance in the former (100% post-EP3) than in the latter (27% to 60%). These pseudo-bud structures induced by  $\beta$ -catenin(RNAi) show low *HySp5-3169*:GFP/GFP expression in the epidermis but high in the gastrodermis, in contrast to what is observed in natural buds (**Figure 2E-2H**). This localized high level of *Sp5* might explain why these pseudo-bud structures do not differentiate hypostome or tentacle rings. These results again point to a differential regulation of *HySp5-3169*:GFP by  $\beta$ -catenin signaling in the epidermis and gastrodermis.

### 3.7. Negative auto-regulation of *Sp5* in the epidermis

To determine whether the transcription factor *Sp5* regulates its own expression in the epidermal and gastrodermal layers, we knocked-down *Sp5* in *HySp5-3169*:GFP transgenic animals and monitored changes in *GFP*, *Wnt3* and *Sp5* expression as well as changes in GFP fluorescence at different time points after EP1 and EP2. We anticipated that after *Sp5*(RNAi) *GFP*/GFP expression would be increased if *Sp5* autoregulation is negative, and decreased if *Sp5* autoregulation is positive. As previously reported, we however noticed some unspecific EP-induced increase in transcript levels when transgenic animals are exposed to scramble siRNAs. Here, this corresponds to an unspecific increase in *Wnt3* levels in both layers, which is maximal in the body column at 8 hours post-EP1 and post-EP2. For *Sp5*(RNAi) *HySp5-3169*:GFP transgenic animals, we did not detect by qPCR analysis

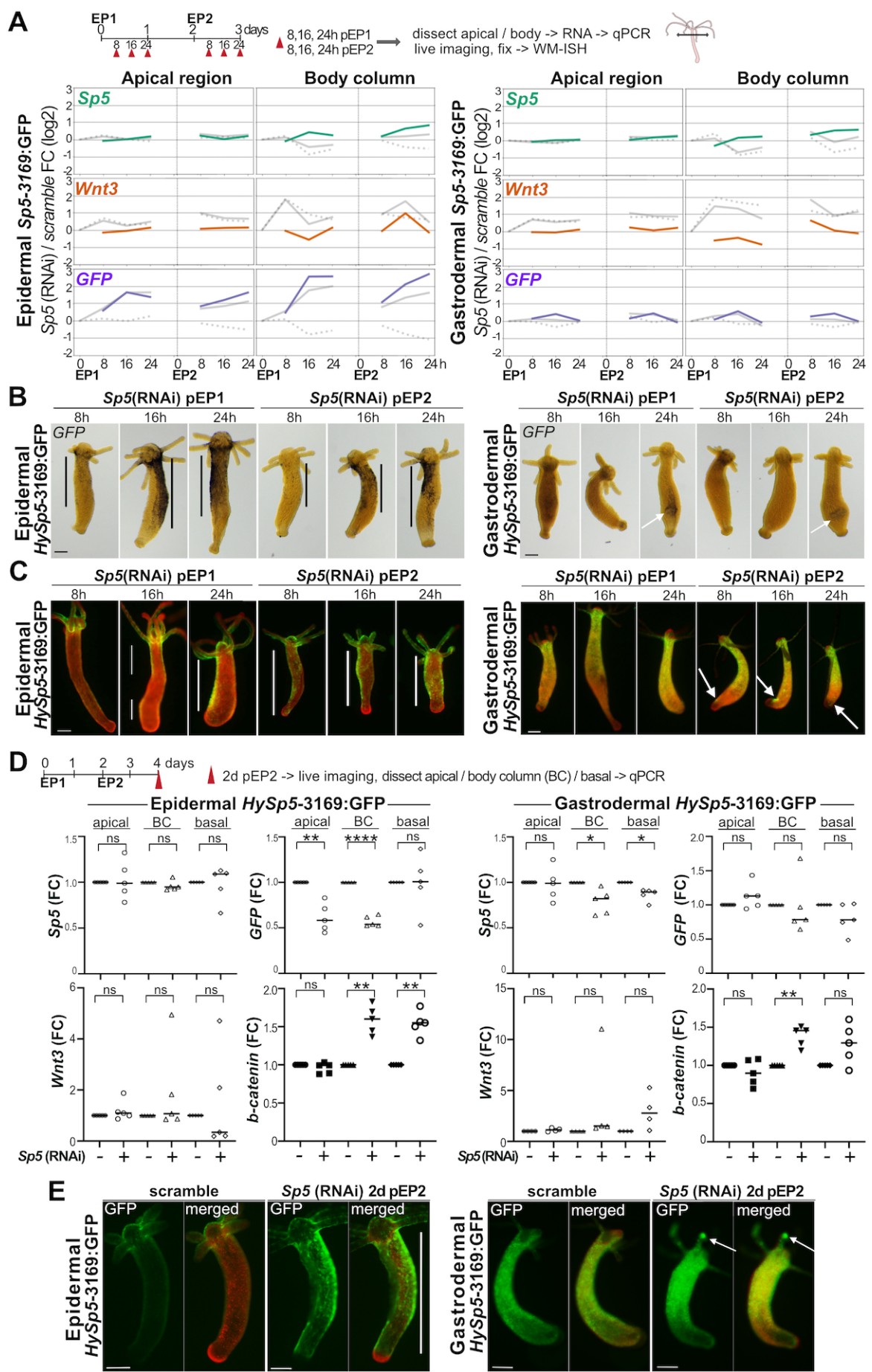


**Figure 5. Ectopic GFP expression in *HySp5-3169:GFP* animals knocked-down for *Sp5*.**

(A) Schematic view of the RNAi procedure applied in experiments depicted in panels A, B, C. At 8h, 16h, 24h post-EP1 (pEP1) and 8h, 16h, 24h post-EP2 (pEP2, red triangles), animals were either fixed for RNA extraction, or fixed for whole mount ISH, or imaged live. Q-PCR analysis of *Sp5*,  $\beta$ -catenin and GFP transcript levels in apical (100%-80%, left) and body column (80%-0%, right) regions of epidermal (left) and gastrodermal (right) *HySp5-3169:GFP* transgenic animals exposed to scramble siRNAs or to *Sp5* siRNAs. In each panel, the colored line corresponds to the Fold Change (FC) values between *Sp5* RNAi animals (continuous grey lines) and control animals exposed to scramble siRNAs (dotted grey lines), which are each expressed as FC relative to non-electroporated animals at time 0, just before EP1. See [Figure S13](#). (B) GFP expression detected by WM-ISH at indicated time-points after *Sp5* (RNAi) as depicted in (A). Vertical black bars along the body column and white arrows in the lower body column indicate regions where GFP is up-regulated. See [Figure S14](#). (C) GFP (green) and mCherry (red) fluorescence in *Sp5* (RNAi) epidermal (left) or gastrodermal (right) *HySp5-3169:GFP* animals as depicted in (A). See [Figure S15](#). (D) Schematic view of the RNAi procedure applied in experiments depicted in panels D and E. Q-PCR quantification of *Sp5*, GFP, *Wnt3* and *b-catenin* transcripts in the apical (100%-80%), central body column (BC, 80%-30%) and basal (30%-0%) regions of epidermal (left) and gastrodermal (right) *HySp5-3169:GFP* animals dissected two days post-EP2 (2d pEP2). (E) GFP (green) and mCherry (red) fluorescence in epidermal (left) or gastrodermal (right) *HySp5-3169:GFP* animals 2d pEP2. White bars indicate areas of ectopic GFP fluorescence along the body column, white arrows spots of ectopic gastrodermal GFP fluorescence here in tentacles. See [Figures S16](#). Scale bars correspond to 250  $\mu$ m except in (B) where it is 200  $\mu$ m.

any significant modulation of *Wnt3* and *Sp5* transcript levels, neither in the epidermal nor in the gastrodermal line. Notably, we found the epidermal *HySp5-3169:GFP* transcripts to be more abundant 16 and 24 hours after EP1 and EP2, two- to four-fold in the apical region, above four-fold in the body column ([Figure 5A](#), [Figure S13](#)).

The analysis of the GFP expression pattern in *Sp5*(RNAi) epidermal *HySp5-3169:GFP* transgenic animals confirmed the above result, with an increase in GFP levels at the same time-points ([Figure 5B](#), [Figure S14A](#)). At the protein level, we first noted at 8 hours post-EP1 some weak epidermal GFP fluorescence along the body column of some control and *Sp5*(RNAi) animals, possibly linked to the EP-induced activation of the *HySp5-3169* promoter. At 16 hours post-EP1, we recorded a marked and specific increase in epidermal GFP fluorescence along the body column of *Sp5* (RNAi) animals, which is maintained high up to 24 hours post-EP2 ([Figure 5C](#), [Figures S15A](#)). However, at two days post-EP2, when the ectopic epidermal GFP fluorescence is still detected, we found the GFP transcript levels in *Sp5*(RNAi) epidermal *HySp5-3169:GFP* transgenic animals significantly reduced in the apical and body column regions, implying that the *Sp5*(RNAi)-induced upregulation of *HySp5-3169:GFP* is transient ([Figure 5D](#)). In gastrodermal *HySp5-3169:GFP* animals, we did not detect global or localized modulation of GFP expression after *Sp5* (RNAi) ([Figure 5A](#), [5B](#), [Figure S13B](#), [S14B](#)). We also did not record any significant change in GFP fluorescence after EP1 ([Figure 5C](#), [Figure S15B](#)). However, after EP2, we noted in about half of the animals ectopic spots of GFP fluorescence, in the lowest part of body column or in the tentacles, indicating that *Sp5* negative autoregulation might also take place in the gastrodermis albeit more spatially-restricted than in the epidermis.

### 3.8. Upregulation of $\beta$ -catenin after *Sp5* (RNAi) in epidermis and gastrodermis

We also performed concomitant q-PCR analysis of *Sp5*, *Wnt3* and  $\beta$ -catenin transcript levels in *HySp5-3169:GFP* animals knocked-down for *Sp5* at two days post-EP2. In epidermal *HySp5-3169:GFP* animals, we detected a significant increase in  $\beta$ -catenin transcripts in the body column and basal regions in the absence of significant modulations of *Sp5* and *Wnt3* levels ([Figure 5D](#)). In gastrodermal *HySp5-3169:GFP* animals, we likewise noted a significant increase in the levels of  $\beta$ -catenin transcripts in these two regions, alongside a slight reduction in the *Sp5* and GFP transcript levels ([Figure 5D](#)). This up-regulation of  $\beta$ -catenin upon *Sp5* (RNAi), which is detected along the body column at a similar extent in both layers, is expected since the negative regulation played by *Sp5* on *Wnt*/ $\beta$ -catenin expression is reduced when *Sp5* is downregulated, even transiently. Such regulation is how-

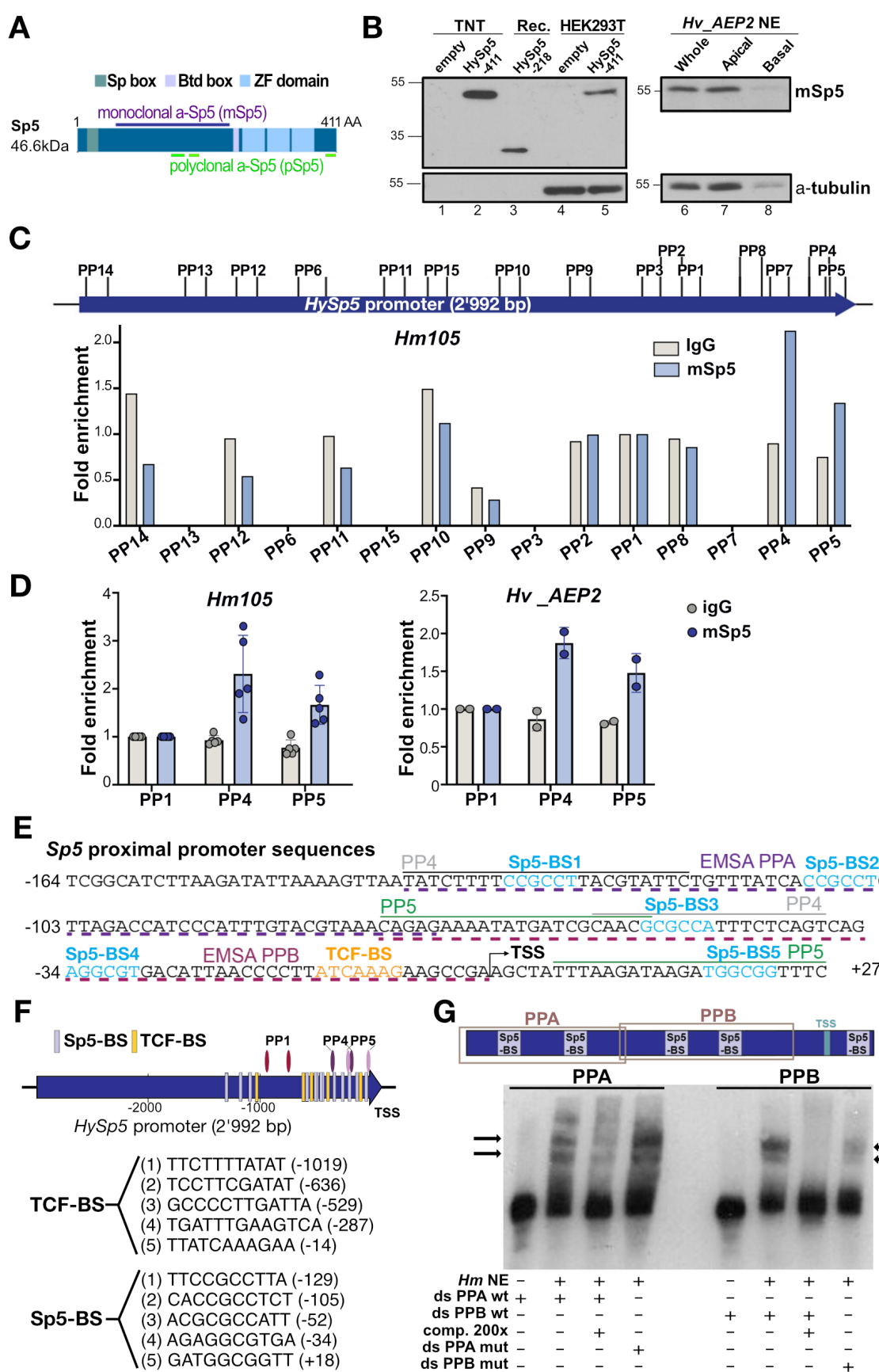


**Figure 6. ChIP-qPCR identification of Sp5-binding sites in the *Hydra* Sp5 promoter.** (A) Structure of the *Hydra* Sp5 protein with the conserved Sp box (green), Buttonhead box (Btd, light purple) and zinc-finger (ZF) domain (light blue); the purple line indicates the 218 AA-long region used to raise the monoclonal anti-Sp5 (mSp5) antibody, the green lines indicated the peptides used to raise the

polyclonal anti-Sp5 (pSp5) antibody. **(B)** Western blot using the mSp5 antibody to detect the TNT-produced HySp5 protein (lanes 1, 2), the HySp5-218 recombinant protein used to raise mSp5 (lane 3), HySp5 expressed in HEK293T cells (lanes 4, 5), or HySp5 present in *Hv\_AEP2* nuclear extracts prepared from whole animals (lane 6), from apical (100%-50%, lane 7) and basal (50%-0%, lane 8) halves. **(C)** Schematic view of the 15 regions (see 15 pairs of primers in **Table S2**) tested along the 2'992 bp-long *Sp5* promoter by ChIP-qPCR using *Hm105* extracts and the mSp5 antibody. A significant enrichment is noted only in regions PP4 and PP5. **(D)** Similar ChIP-qPCR enrichment in regions PP4 and PP5 obtained with mSp5 antibody when *Hm105* (left) or *Hv\_AEP2* (right) extracts are used. See **Figure S17**. **(E)** Proximal *HySp5* promoter sequence (-162 to +29), which contains the transcriptional start sites (TSS) identified in *Hv\_AEP* (TSS1 +1) and *Hm105* (TSS2 -149, see **Figure S18**), five Sp5 binding sites (SP5-BS, light blue), a single TCF binding site (TCF-BS, orange), the PP4 (grey) and PP5 (green) primers used for ChIP-qPCR. In the same region, the PPA (-135 to -67) and PPB (-71 to +2) stretches, underlined with purple (PPA) and pink (PPB) dashed lines respectively, were used in Electro-Mobility Shift Assay (EMSA). **(F)** Schematic map of the *HySp5* 2'992 bp promoter region indicating the predicted TSS1, the clustered TCF-BS and Sp5-BS (light purple and orange bars respectively), the PP1, PP4 and PP5 primer pairs. Sequences of the TCF-BS and Sp5-BS identified in the *HySp5* promoter. **(G)** EMSA showing a shift of the PPA and PPB ds-DNAs incubated with *Hm105* NEs. Comp.: unlabeled ds-PPA (left) or ds-PPB (right) added as competitor 200x in excess during the incubation; mut: mutated.

ever not detected in the apical region, consistently with previous results (Vogg et al. 2019).

Despite the lack of sustained down-regulation of *Sp5* transcripts after *Sp5*(RNAi), we conclude that the two-step RNAi procedure we applied is effective, highlighting the dynamic regulation of *Sp5* in each epithelial layer, with a 24 hour-long lasting up-regulation of *HySp5-3169:GFP* along the epidermis after each exposure to *Sp5*(RNAi). We did not record such modulation of *HySp5-3169:GFP* in the gastrodermis. We interpret the upregulation of epidermal *GFP* transcripts after *Sp5*(RNAi) as the consequence of knocking down the negative autoregulation played by the *Sp5* transcription factor on its own expression. This is however only transient, as one day later, the *GFP* expression levels decrease by about twofold, probably as a consequence of the up-regulation of *β-catenin* expression that takes place in both layers of the body column, leading to a transient up-regulation of *Sp5* between 24 and 48 hours after EP2, producing *Sp5* protein at a level where it represses the *Sp5* promoter, and hence decreases *GFP* transcript levels. However, two days after EP2, an ectopic *GFP* fluorescence is still visible in the epidermis (**Figure 5E**, **Figure S16**), in keeping with the long lifespan of the *GFP* protein [43].

### 3.9. Identification of five active *Sp5*-binding sites within the proximal *Hydra Sp5* promoter

The *Hydra Sp5* transcription factor belongs to the Sp/KLF family, a class of DNA-binding proteins that bind GC-rich boxes or GT/CACC elements through their three zinc finger (ZF) domains [32,44]. We previously identified by ChIP-seq analysis performed with extracts from HEK293T cells five Sp5 binding sites (Sp5-BS) and five TCF binding sites (TCF-BS) within 2'966 bp of the *Sp5* promoter, clustered in two adjacent regions named PPA and PPB in the vicinity of the *Sp5* transcriptional start site [33]. To identify active Sp5-binding sites (Sp5-BS) within the *Hydra Sp5* promoter sequences, we raised antibodies against the *Hydra Sp5* protein with the aim to perform a ChIP-qPCR analysis of the *HySp5* promoter using *Hydra* extracts and to compare the Sp5-binding sites with those previously identified in human cells expressing HySp5. We raised two antibodies against HySp5, one monoclonal and one polyclonal, designed to target regions that do not overlap with the evolutionarily conserved domains present in HySp5, the Sp box, the Buttonhead-box and the ZF DNA-binding domain (**Figure 6A**, **Figure S17A**). The two Sp5 antibodies specifically recognize the Sp5 protein, either as HySp5-218 recombinant protein (24.5 kDa) used to raise the Sp5 monoclonal antibody or produced full length *in vitro* with the TNT reticulocyte transcription-coupled-translation system, or expressed in transfected HEK293T cells (**Figure 6B**, **Figure S17B,17C**).

In *Hv\_AEP2* extracts, the monoclonal anti-Sp5 detects the Sp5 protein at higher levels in the apical region than in the body column as expected. By contrast, in three independent

experiments, the polyclonal anti-Sp5 antibody recognizes a band at the appropriate size but exclusively in nuclear extracts (NEs) prepared from the lower body column and not from the apical region (**Figure S17C**). To evidence a possible cross-reactivity with the closely related Sp4 protein, we tested the polyclonal  $\alpha$ -Sp5 antibody on the TNT-produced *Hydra* Sp4 protein but did not detect any band. We suspect that the polyclonal  $\alpha$ -Sp5 antibody detects the Sp5 protein but also cross-reacts with an unidentified Sp/KLF protein predominantly expressed in the body column and basal half of *Hydra*.

Next, we tested both the monoclonal and the polyclonal  $\alpha$ -Sp5 antibodies in ChIP-seq analysis of the Sp5-bound regions. We first used *Hm-105* extracts to assay the amplification of 15 regions along the 3'169 bp of the *Sp5* promoter and 5'UTR sequences after ChIP (**Figure 6C**, **Figure S17D**). Among these 15 regions, we found only two 100 bp-long regions specifically enriched with one or the other antibody but not by the pre-immune serum, i.e. the overlapping PP4 (-135 / -36) and PP5 (-71 / +29) regions, located in the *Sp5* proximal promoter. We noted a similar enrichment in regions PP4 and PP5 by ChIP-qPCR with extracts from *Hv\_AEP* animals (**Figure 6D**, **Figure S17D**). These two regions were also identified when the ChIP-qPCR analysis was performed with extracts from human cells expressing HySp5 [33]. Each region contains three putative Sp5-BS, one of them (Sp5-BS3) being present in both PP4 and in PP5 (**Figure 6E, 6F**).

To test whether these putative Sp5-BS are functional in *Hydra*, we designed two double-stranded oligonucleotides (ds-DNAs) to perform Electro-Mobility Shift Assay (EMSA) with (1) PPA (-135 to -67) that encompasses the identical Sp5-BS1 and Sp5-BS2 motifs, and (2) PPB (-71 to +2) that contains the distinct Sp5-BS3 and Sp5-BS4 motifs (**Figure 6E-6G**). When *Hydra* NEs were incubated with biotin-labeled Sp5 ds-DNAs, we recorded a mobility shift, with two retarded bands for PPA and two distinct bands for PPB, no longer visible in the presence of a 200x excess of unlabeled oligonucleotides (**Figure 6G**). Mutation of Sp5-BS1 and Sp5-BS2 in the PPA region (CCGCCT  $\rightarrow$  CTTCCCT) did not cancel the shift, but rather accentuated it. In contrast, when Sp5-BS3 (GCGCCA  $\rightarrow$  GTTCCA) and Sp5-BS4 (AGGCCT  $\rightarrow$  ATTCTG) in the PPB region were mutated, the shift almost disappeared. We therefore concluded that HySp5 likely binds the putative Sp5 binding sites in the PPA and PPB regions, with higher specificity in the latter; these results support the hypothesis that in *Hydra*, the Sp5 transcription factor is involved in *Sp5* autoregulation.

### 3.10. The *Sp5* proximal promoter is involved in *Sp5* negative autoregulation

To determine whether some of these five proximal Sp5 binding sites are indeed involved in Sp5 auto-regulation, we tested these sequences in an *ex vivo* transactivation assay system (**Figure 7A**). We prepared seven reporter constructs where the expression of luciferase is driven either by the full *HySp5* promoter (*HySp5-2992: luciferase*), or by a shorter version where 164 bp of the proximal sequences are deleted (*HySp5-2828: luciferase*), or by the full *HySp5* promoter where one of the five *HySp5-BS* is mutated (*HySp5-2992-mBS1: luciferase*, -mBS2, -mBS3, -mBS4, -mBS5). Each of these reporter constructs were co-expressed in HEK293T cells either with the full Sp5 protein under the control of the CMV promoter (CMV:HySp5-420), or with a truncated version of the Sp5 protein lacking the DNA-binding domain (CMV:HySp5- $\Delta$ DBD).

In conditions where Sp5 is either not expressed or expressed but in its truncated version (*HySp5- $\Delta$ DBD*), we recorded a low luciferase activity, consistent with the fact that the *HySp5-2992* promoter is poorly active in HEK293T cells (Vogg et al., 2019). By contrast, in the presence of *HySp5-420* protein, we measured a 7x higher activity of the *HySp5-2992* promoter, and obtained similar levels when the *HySp5-BS1*, *HySp5-BS2* and *HySp5-BS4* sites are mutated (**Figure 7A**). However, surprisingly, when the proximal sequences are completely deleted, the transactivation levels are more than doubled, indicating that these sequences actively repress the activity of the *HySp5-2992* promoter in the presence of *HySp5-420* protein. When the *HySp5-BS3* and *HySp5-BS5* sites are mutated, the activity is lower than that recorded when the *HySp5-2992* promoter is complete, indicating that either these two sites play a positive role for the full activity of the *HySp5* promoter, or they

restrict the repressive activity of the proximal sequences. These results show that the *HySp5* promoter is submitted to a complex regulation, with a clear *Sp5*-dependent repressive role of the proximal sequences, and an enhancing role of the more upstream ones.

### 3.11. The *Zic4* transcription factor positively regulates *Sp5* expression

We recently showed that the *Hydra* transcription factor *Zic4* (*HyZic4*), which is involved in the differentiation of tentacles and the maintenance of their identity, is a downstream target gene of *HySp5* [34]. We considered the possibility that *Zic4* also regulates *Sp5* expression in a feedback loop. We first searched for the presence of *Zic*-binding sequences (*Zic-BS*) as deduced from those identified in vertebrate or non-vertebrate gene promoters [45] (Table 1). We identified two putative *Zic-BS* in the *HySp5*-2992 upstream sequences at positions -670/-659 and -391/-369 (Table 1, Figure S2), as well two putative *Zic-BS* in the *HyWnt3*-2149 upstream sequences and five in the *HyZic4* ones (Table 1, Figure S19). To test whether *HyZic4* regulates *HySp5*, we expressed in HEK293T cells the *HySp5*-2992:Luciferase construct together with either the full *HyZic4* protein (CMV:Zic4-431) or a truncated form lacking its DNA-binding domain (CMV:HyZic4-ΔDBD) (Figure 7B). In the presence of *HyZic4*, the *HySp5*-2992:Luciferase activity is multiplied by almost 50x when human  $\beta$ -catenin is co-expressed and over 50x when human  $\beta$ -catenin is not co-expressed. Remarkably, Luciferase activity becomes basal when the *Zic4* DNA-binding domain is deleted, indicating that *HyZic4* is able to enhance *HySp5* expression through direct binding to its promoter, independently of  $\beta$ -catenin.

Species	Target genes	Zic TF	ZIC binding-site sequence	References
Mm	<i>Gli</i> - consensus	Zic1-5	TGGGTGGTC	[46,47]
Mm	<i>Lamin A/C</i>	Zic1	CCACCCCT	[48]
Mm	<i>Math1</i>	Zic1	GCTCCCCGGGGAGCT	[49]
Mm	<i>ApoE</i> _A	Zic1/2	GGACTGTGGGGGGTGGTCAA	[50]
	_B		AAACTGTGGGGGGTGGTCAA	
	_C		GGACTGTGGGGGGTGAAAAAA	
	_D		CTATCCCTGGGGGAGGGGGC	
Hs	<i>D1A</i>	ZIC2	CCCCCAGGGCA	[51]
Mm	<i>CamK II</i>	Zic2	GTGTGGGC	[52]
Mm	<i>Pax3</i>	Zic2	CTGCTGGGG	[53]
Mm	<i>Oct4</i>	Zic2	2550 ~ -2430	[54]
Hs	$\alpha$ - <i>ACTIN</i>	ZIC3	GGAGGG	[55]
Mm	<i>Nanog-C, Nanog-T</i>	Zic3	CC (C/T) GCTGGG CCTGCTGGG	[56]
Hs	<i>E-CADHERIN (CDH1)</i>	ZIC5	-283 ~ -71	[57]
Ci	<i>Brachyury</i>	ZicL	CCAGCTGTG	[58]
Ci	<i>E(SPL)/HAIRY-B</i>	Macho1	5' -GCCCGCCGCTG-3'	[59]
Hr	<i>synthetic</i>	Macho1	GACCCCCCA	[60]
Hv	- 672	Zic	AACCTGGCCTGC	[33,34]
	- 383		GGCAGGTGCCGGC	<i>this work (Figure 7, S2)</i>
Hv	- 1781	Zic	GCCCCGCGCTCTCC	[27,33]
	- 1177		GACAGCGGGTG	<i>this work (Figure 7, S19A)</i>
Hv	<i>Sp5</i>	Zic	ATCGCCCCCTCTCGCT	[34]
	- 1863		ACGGGCATTGGCGTGA	<i>this work (Figure 7, S19B)</i>
	- 1825		GAGGTGACCCATGCTG	<i>this work (Figure 7, S19B)</i>
	- 1736		AGGAAAGGGGTGCTACA	<i>this work (Figure 7, S19B)</i>
	- 1291		TGCTCCCGT, TACCCCGCTA	<i>this work (Figure 7, S19B)</i>
	- 107, + 77			

**Table 1. Zic-binding sites in chordates and in the upstream sequences of the *Sp5*, *Wnt3*, *Zic4* *Hydra* genes.** Ci: *Ciona intestinalis* (ascidian), Hr : *Halocynthia roretzi* (ascidian), Hs: *Homo sapiens*, Hv : *Hydra vulgaris*, Mm: *mus musculus*.

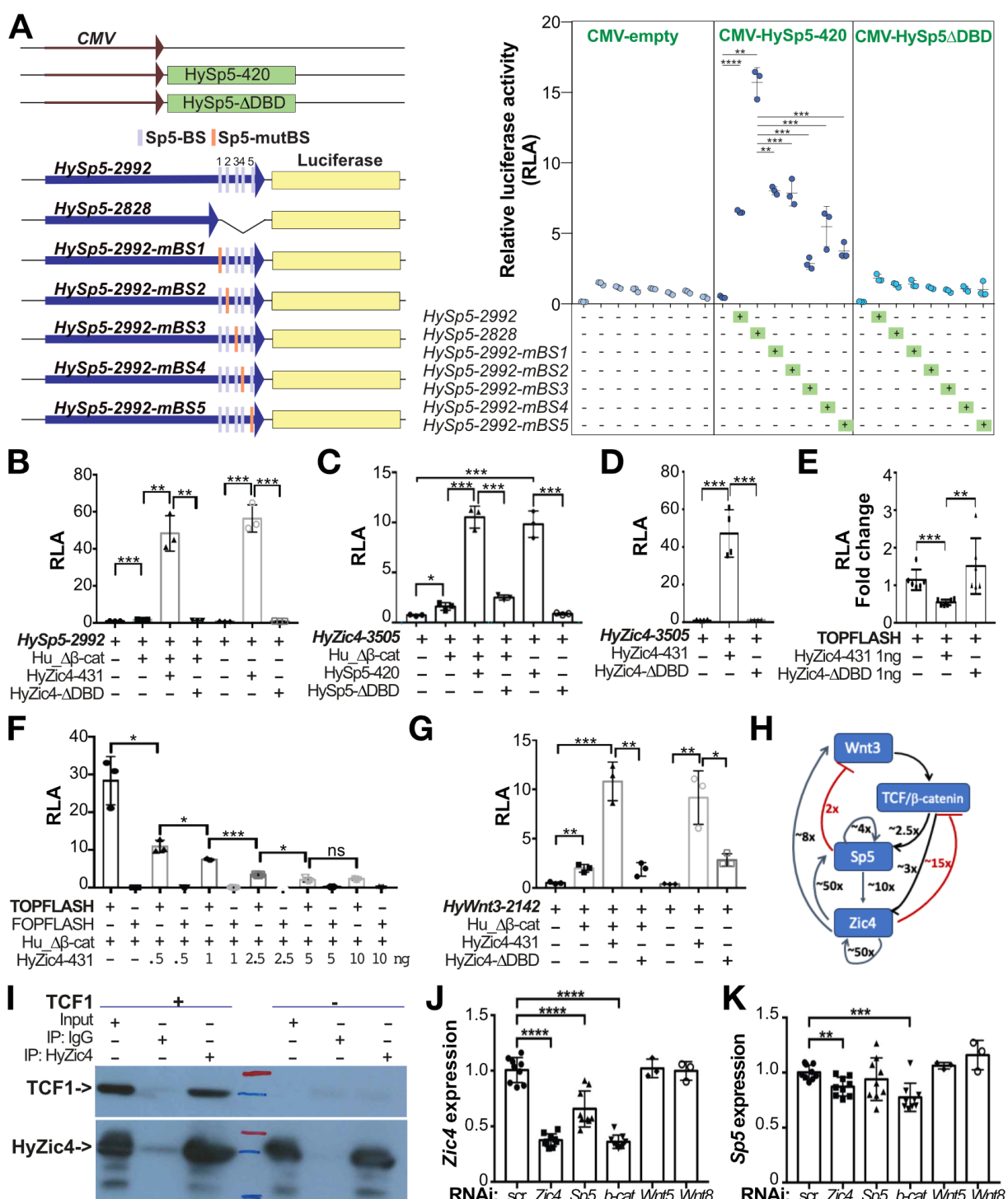


**Figure 7. Functional analysis of the *Hydra* *Sp5*, *Zic4* and *Wnt3* promoters.** (A-G) Luciferase reporter assays performed in HEK293T cells to measure the Relative Luciferase Activity (RLA) driven by various promoters when *Hydra* proteins are co-expressed. Each data point represents one biological independent experiment. (A) RLA levels driven by the *HySp5* promoter when 2'992 bp long, or when deleted of its proximal region (*HySp5*-2828) that contains five Sp5 binding sites (Sp5BS), or when one of these 5 Sp5BS is mutated (mBS1, mBS2, ...). Each construct was tested in the absence of any protein co-expressed (CMV-empty), or the presence of co-expressed full-length Sp5 (*HySp5*-420) or Sp5 lacking its DNA-Binding Domain (*HySp5*-ΔDBD). (B) RLA levels driven by the *HySp5*-2992 promoter when the full-length HyZic4 (*HyZic4*-431) or the truncated HyZic4 lacking its DNA-Binding Domain (*HyZic4*-ΔDBD) are co-expressed. (C, D) RLA levels driven by the *HyZic4*-3505 promoter when full-length or truncated HySp5 (*HySp5*-420, *HySp5*-ΔDBD in C) or full-length or truncated HyZic4 (*HyZic4*-431, *HyZic4*-ΔDBD in D) are co-expressed. (E, F) RLA levels driven by the TOPFlash or FOPFLASH reporter constructs that contain 6x TCF binding sites either consensus

847  
848  
849  
850  
851  
852  
853  
854  
855  
856  
857  
858  
859

or mutated when HyZic4-431 (E, F) or HyZic4-ΔDBD (E) are co-expressed. **(G)** RLA levels driven by the *Wnt3*-2142 promoter when HyZic4-431 or HyZic4-ΔDBD are co-expressed. **(H)** Schematic view of the regulations detected in HEK293T cells on the *Hydra* *Wnt3*, *Sp5* and *Zic4* upstream sequences when the human  $\beta$ -catenin and/or HySp5, HyZic4 proteins are co-expressed (this work, Vogg et al. 2019, Vogg et al. 2022). **(I)** Immunoprecipitation (IP) of HA-tagged HyZic4-431 expressed in HEK293T cells together or not with huTCF1. IP was performed with an anti-HA antibody and co-IP products were detected with the anti-TCF1 antibody. Same results were obtained in two independent experiments. **(J, K)** *Zic4* (J) and *Sp5* (K) transcript levels measured by qPCR in *Hv\_Basel* animals exposed twice to scrambled (scr) sRNAs or *Zic4*, *Sp5*,  $\beta$ -catenin (*b-cat*), *Wnt5* or *Wnt8* siRNAs. Levels are normalized to those measured in control animals exposed to scr sRNAs. In all panels, error bars indicate Standard Deviations and statistical p values are as follows: \*p  $\leq$  0.05, \*\*p  $\leq$  0.01, \*\*\*p  $\leq$  0.001, \*\*\*\*p  $\leq$  0.0001 (unpaired t test).

Next, we tested in HEK293T cells the level of *HyZic4* promoter activity, which contains two putative Sp5 binding sites [34], when Sp5 is co-expressed. We measured a 10x increase in *HyZic4*-3505: luciferase activity when the full Sp5 protein (CMV:HySp5-420) is co-expressed, an increase no longer detected when the Sp5 protein lacks its DNA-binding domain (CMV:HySp5-ΔDBD) (**Figure 7C**). As previously, this increase is observed at similar levels in the presence or absence of human  $\beta$ -catenin co-expression. This result indicates that Sp5 can significantly enhance *HyZic4* expression through direct DNA-binding.

Similarly, we also measured a strong Zic4 auto-activation (~50x), which requires the DNA-binding domain (**Figure 7G**). By contrast, when we used the TOPFlash assay where six tandem TCF-binding sites can enhance luciferase expression [61], we found the TOPFLASH luciferase activity decreased when Zic4 is co-expressed. This Zic4-dependent repression requires the Zic4 DNA-binding domain, proved to be Zic4 dose-dependent and is enhanced when human  $\beta$ -catenin is co-expressed (**Figure 7E, 7F**). However, when we tested the Zic4 activity on the *Wnt3* promoter (2'142 bp), we found a 10x increase in *HyWnt3*-2142: luciferase activity, likely through a direct interaction as this increase is no longer observed when the Zic4 DNA-binding domain is deleted (**Figure 7G**).

We have summarized these interactions with those previously identified with Sp5 or Zic4 in HEK293T cells [28,29] in a scheme that presents a series of positive loops where Zic4 appears very potent, including in its own autoregulatory loop, and two negative regulations, with Sp5 repressing *Wnt3* expression, and Zic4 repressing TCF-regulated promoters (**Figure 7H**). In HEK293T cells overexpressing *HyZic4*, we also show by co-immunoprecipitation that the two transcription factors HyZic4 and human TCF1 can physically interact (**Figure 7I**), similarly to what we previously showed between HySp5 and TCF1 [33]. These results suggest that in *Hydra* cells where Sp5 and Zic4 are co-expressed, they enhance each other's expression while repressing TCF/ $\beta$ -catenin transcriptional activity.

We tested this gene regulatory network (GRN) in *Hydra* and indeed found in animals knocked-down for Zic4 or  $\beta$ -catenin the Zic4 levels down-regulated at least two-fold, also reduced after Sp5 knocked-down but at a lower level (**Figure 7J**). We also found the levels of Sp5 moderately down-regulated in animals knocked-down for Zic4 or for  $\beta$ -catenin (**Figure 7K**). We concluded that the regulatory events recorded in HEK293T cells likely take place in *Hydra* cells where all components of this GRN are expressed, namely in the gastrodermal epithelial cells of the head region where Sp5 and Wnt3 are highly expressed, and in the epithelial battery cells located in the epidermis of the tentacles (**Figure 8A**).

## 4. Discussion

### 4.1. Epithelial layer-specific regulations of Sp5 in intact animals

To better decipher the dynamics of interactions between the activating and inhibiting components of the head organizer in intact and regenerating *Hydra*, we compared the *in vivo* regulation of Sp5 in each epithelial layer, epidermal and gastrodermal, when developmental, pharmacological or genetic conditions vary (see **Table A1**). For this purpose, we used transgenic lines expressing the reporter construct *HySp5*-3169:GFP either in the

epidermis or gastrodermis and analyzed GFP expression in intact or developing animals, either regenerating or budding. In intact animals, we found several differences between epidermal and gastrodermal *GFP/GFP* expression; in the epidermis *GFP/GFP* is expressed throughout the hypostome, while the tip of the hypostome is free of gastrodermal *GFP/GFP*, in agreement with the fact that *Sp5* transcripts are not detected in this area [33]. In addition, epidermal *GFP/GFP* is maximal in the tentacle ring and uppest body column while the gastrodermal one extends along the body axis. In animals regenerating their heads, we noted a differential temporal regulation of *Sp5* in each layer, with *GFP* up-regulated during the early phase in the gastrodermis but one day later in the epidermis.

These layer-specific regulations of *HySp5-3169:GFP* were identified through different approaches: at the protein level by monitoring *in vivo* GFP fluorescence and immunodetecting GFP protein expression, and at the transcript level by performing qPCR and *in situ* hybridization to quantify and map *GFP* expression along the body axis. In addition, these layer-specific regulation of *Sp5* in intact animals are supported by the single-cell analysis of *Sp5* expression [35] that shows a predominant expression of *Sp5* in epithelial cells, with maximal levels observed in tentacle battery cells located in the epidermis, a lower level in epithelial cells of the hypostome and no expression in stem cells along the body column. In the gastrodermis, single-cell analysis detects the highest levels of *Sp5* in apical cells and in one sub-population of epithelial stem cells along the body column (**Figure 8A**). Therefore, we concluded that the *HySp5-3169:GFP* transgenic lines provide suitable and reliable tools to monitor the endogenous *Sp5* regulation, with the 3 kb of *Sp5* upstream sequences inserted in this construct being sufficient to direct *GFP* expression in a way that mimics endogenous *Sp5* regulation in each layer.

#### 4.2. Three architectures of the *Wnt3/β-catenin/TCF/Sp5/Zic4* GRN in intact *Hydra*

This study adds a new level of understanding of how the head organizer works in *Hydra*. The parallel analysis of the *Wnt3/β-catenin/TCF/Sp5/Zic4* GRN in human HEK293T cells and in *Hydra* epithelial layers reveals complex cross-regulatory interactions. We first could confirm several positive regulations, those of *Wnt3/β-catenin/TCF* on *Sp5* and *Zic4* expression, that of *Sp5* on *Zic4*, and identify some new ones *Zic4* on *Sp5*, *Zic4* on *Wnt3* (at least in HEK293T cells). We also confirm the down-regulation of *Wnt3* by *Sp5* and report as a new finding the down-regulation of *β-catenin* by *Sp5*, as well as the down-regulation of *β-catenin/TCF* activity by *Zic4* (at least in HEK293T cells). Finally, we identify autoregulatory loops, positive for *Sp5/Sp5* and *Zic4/Zic4* in HEK293T cells, positive for *Wnt3/Wnt3* and *β-catenin/β-catenin* via *TCF* in *Hydra*, and negative for *Sp5/Sp5* in *Hydra* epidermis (see **Table A1**).

By analyzing these interactions along the body axis of intact animals, we could characterize three distinct organization of the *Wnt3/β-catenin/TCF/Sp5/Zic4* GRN that correspond to three distinct patterning functions in three anatomical contexts (**Figure 8**). Indeed, the analysis of *Wnt3*, *β-catenin*, *Sp5* and *GFP* regulation in epidermal and gastrodermal *HySp5-3169:eGFP* and *HyWnt3-2149:eGFP* transgenic lines after ALP treatment, *β-catenin(RNAi)* or *Sp5(RNAi)* shows that *Sp5* is differentially regulated in the epidermis and gastrodermis (1) *at the apex*, (2) *in the tentacle zone*, (3) *along the body column* (**Figure 8B-8E**). At the apex of intact animals, the tightly spatially restricted expression of *Sp5* in the gastrodermis is crucial for maintaining maximal levels of *Wnt3* expression at the tip of the head, where *Wnt3/β-catenin/TCF* signaling drives the constitutive head organizer activity leading to head maintenance. In the tentacle zone, the positive co-regulation of *Sp5* and *Zic4* in the epidermis of the tentacle zone is critical for tentacle formation with an unclear role for the gastrodermis. Along the body column, the high levels of *Sp5* expression and *Sp5* activity in the gastrodermis, possibly through positive autoregulation, are critical for keeping *Wnt3/β-catenin/TCF* signaling low and preventing the formation of ectopic tentacles or ectopic heads.

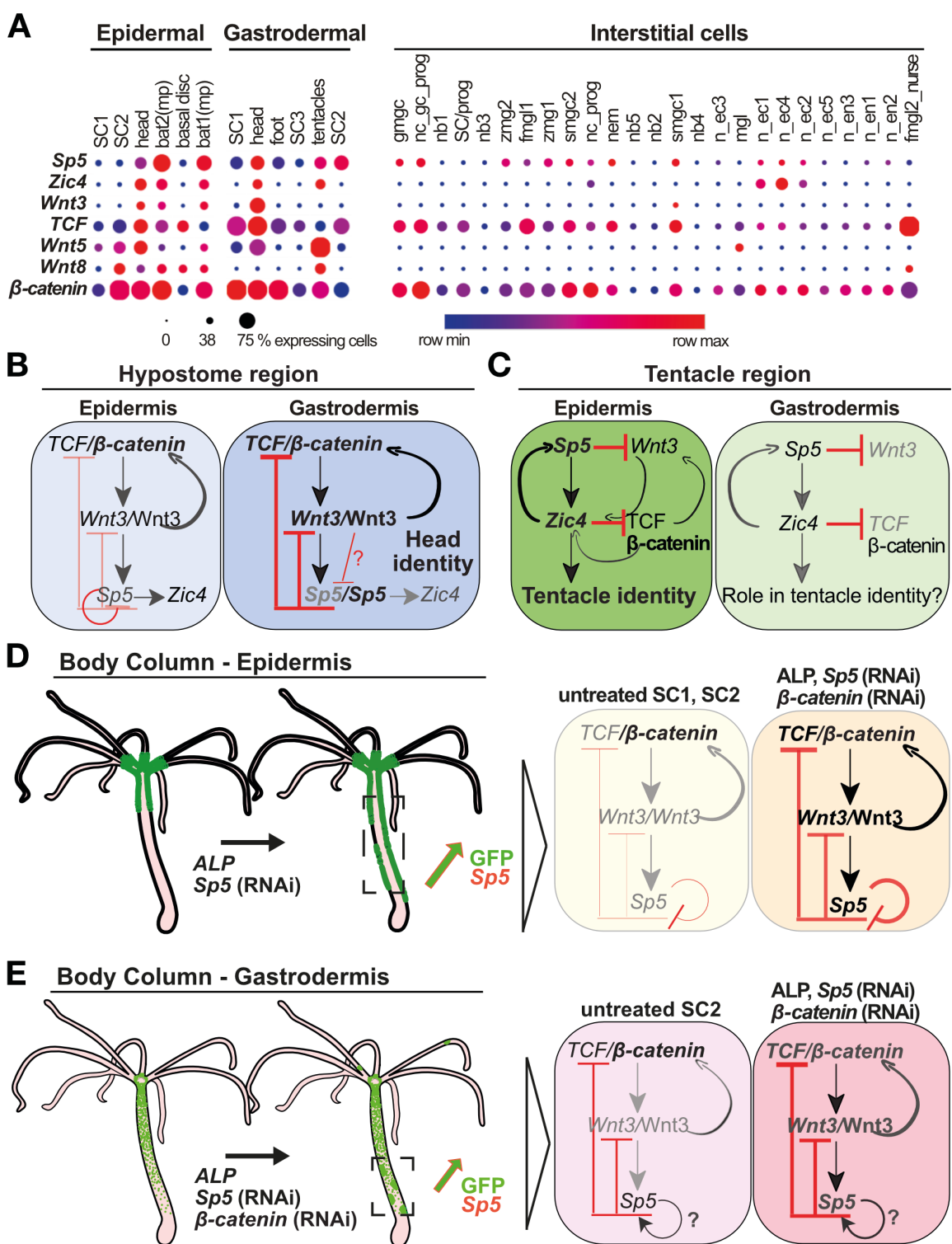


Figure 8: Schematic summary of the layer-specific *Sp5* regulation along the *Hydra* body axis.

**(A)** Dot plot view of *Zic4*, *Wnt3*, *Sp5*, *TCF*, *Wnt5A*, *Wnt8* and  $\beta$ -catenin expression in cells from the epithelial lineages, either epidermal or gastrodermal, and the interstitial lineage as deduced from *Hydra* single-cell transcriptome analysis (Siebert et al, 2019). Along the central body column, single cell sequencing has identified two populations of epithelial stem cells in the epidermis (SC1, SC2) and three in the gastrodermis (SC1, SC2, SC3). See other abbreviations in **Figure S1**. **(B, C)** Schematic representation of the predicted genetic regulation network (GRN) at work in the epidermal and gastrodermal layers of the head (B) and tentacle (C) regions in *Hydra*. **(D, E)** Schematic view of GFP fluorescence, *Sp5* expression and predicted GRNs at work in the epidermal (D) and gastrodermal (E) layers of the body column (BC) of *HySp5-3169:GFP* transgenic animals, either maintained in homeostatic conditions (left), or ALP-treated / knocked-down for *Sp5* or  $\beta$ -catenin (right).

#### 4.3. Diffuse *Sp5* negative autoregulation in the epidermis

*Sp5* was identified as a target and a regulator of the Wnt transcriptional program in vertebrates [28–32], notably as a repressor [30,62]. We also showed that *Hydra* or zebrafish *Sp5* expressed in human cells act as evolutionarily conserved transcriptional repressors, including on the transcriptional machinery and on *Sp* genes [33]. This study confirms this finding as in *Hydra*, *HySp5* negatively regulates its own expression in the epidermis, as evidenced by the transient up-regulation of *Sp5* after each exposure to *Sp5* siRNAs. However, the response to *Sp5*(RNAi) in *HySp5-3169*:GFP transgenic animals is highly asymmetrical between the epithelial layers, with in the epidermis, a transient but massive increase in *GFP* expression and *GFP* fluorescence along the body axis, together with a limited increase in *Sp5* and *Wnt3* levels along the body column. In contrast, in the gastrodermis, we recorded no overall increase in *GFP* transcript level, but only a few ectopic spots of *GFP* overexpression or *GFP* fluorescence in the peduncle region and tentacles.

We interpret this transient *GFP/GFP* upregulation in the epidermis together with that of *Sp5* although more limited, as a release of the negative auto-regulation played by *Sp5* in this layer. This epidermal-specific *Sp5* negative autoregulation suffices to explain the lower constitutive *Sp5* expression recorded in this layer. As such, this constitutive asymmetry in *Sp5* expression also explains the more effective *Sp5*(RNAi) knock-down in the epidermis as *Sp5* levels are low and epithelial cells highly accessible to electroporated siRNAs, whereas in the gastrodermis *Sp5* levels are higher and epithelial cells less accessible.

Among the 2'992 bp *Sp5* upstream sequences, the ChIP-seq analysis could identify only two areas in the *Sp5* proximal promoter, PPA and PPB, which are enriched in *Sp5* protein when *Hm-105* or *Hv\_AEP2* nuclear extracts are used. In addition, these two areas, which each contain two *Sp5*-binding sites previously identified by ChIP-seq analysis in human cells expressing *HySp5*, are necessary for *Sp5* negative autoregulation. The role of *Sp5* negative autoregulation in the GRN is further supported by the findings showing that *Sp5* can directly regulate its own promoter.

*Sp5* regulation is quite dynamic, as observed in *HySp5-3169*:GFP animals exposed to *Sp5*(RNAi) where *GFP* levels are first found upregulated in the epidermis as discussed above, then one day later significantly down-regulated in the apical region and body column, providing evidence for a return to *Sp5* repressive activity. In parallel, *Sp5* and *Wnt3* transcript levels remain unaffected, possibly as the result of the highly dynamic cross-regulations that take place between these genes. In the gastrodermis, *Sp5* and *GFP* levels are only mildly decreased in response to *Sp5*(RNAi), whereas *β-catenin* is up-regulated in both layers along the body column indicating that in intact animals *Sp5* acts as a head inhibitor by repressing not only *Wnt3* but also *β-catenin* expression, thus reinforcing the feed-back loop that reduces head activation, i.e. *Wnt3/β-catenin* signaling activity.

#### 4.4. Distinct configurations of the *Wnt3/β-catenin/Sp5* GRN in the homeostatic and developmental head organizers

This study shows that the temporal and spatial regulation of *Sp5* and *Wnt3* in each epithelial layer is in fact different in the homeostatic and developmental organizers. In intact animals, the absence of *HySp5-3169*:GFP expression in the gastrodermal epithelial cells of the perioral region where *Wnt3* expression is maximal, indicates that a high level of Wnt/β-catenin signaling can only be stably maintained if *Sp5* expression is repressed. This equilibrium situation is necessary to maintain homeostatic organizer activity. How *Sp5* expression is maintained inhibited within gastrodermal cells of the homeostatic head organizer has not yet been identified. Since in each context where *Wnt3* expression is highest, *Sp5* is repressed, we infer that the highest levels of Wnt/β-catenin signaling induce transcriptional repression of *Sp5* and/or degradation of *Sp5* transcripts.

In contrast, in the apical-regenerating tip, the *Sp5* expression domain is broad in the gastrodermis, necessary for restricting head organizer activity, i.e. *Wnt3* and *β-catenin* up-regulation as well as activation of Wnt3/β-catenin/TCF signaling, as such as a single head develops instead of multiple ones. The *Wnt3* and *Sp5* gastrodermal domains overlap at

least for the first 24 hours after mid-gastric bisection, with *Sp5* expressed at a high level in these cells. Therefore, we believe that in gastrodermal epithelial cells that have the power to develop organizing activity as in apical-regenerating tips, *Wnt3/β-catenin* signaling is protected from *Sp5* activity, either by active inhibition of *Sp5* repressive transcriptional activity on *Wnt3* or *β-catenin* expression, or by enhanced degradation of the *Sp5* protein. In conclusion, it remains to be understood how interactions between *Wnt3/β-catenin* signaling and the *Sp5* transcription factor remain distinct in the homeostatic and developmental head organizers, possibly via transcriptional or post-transcriptional mechanisms in the former context, via translational or post-translational mechanisms in the latter one.

#### 4.5. Phenotypic changes induced by dysregulations of the *Wnt3/β-catenin/TCF/Sp5/Zic4* GRN

The perturbations of the dynamic interactions within the *Wnt3/β-catenin/TCF/Sp5/Zic4* GRN induce several phenotypes along the body axis such as the loss of tentacle identity after *Zic4(RNAi)* [34], the formation of ectopic tentacles after ALP treatment [23] associated with an overall increase in gastrodermal *Sp5* expression and a punctuated up-regulation of *Wnt3* in both layers, the formation of multiple ectopic heads induced by *Sp5(RNAi)* linked to the time- and space-restricted decrease in gastrodermal *Sp5* associated with the localised activation of *Wnt3/β-catenin/TCF* signaling as observed in *Hv\_Basel* [33], the formation of pseudo-bud structures induced by *β-catenin(RNAi)* named pseudo-buds as they rarely differentiate a head. This phenotype is highly penetrant in *Hv\_Basel*, present in 100% animals one day after EP3, identical but less penetrant in *Hv\_AEP2* transgenic animals.

The regulations of *Sp5* in *β-catenin(RNAi)* *HySp5-3169:GFP* transgenic animals are layer-specific, consistent with the observed phenotype. In the epidermis, *β-catenin(RNAi)* leads to a drastic reduction in *GFP* expression and *GFP* fluorescence, consistent with the known direct positive regulation of *Sp5* expression by *Wnt/β-catenin* signaling [33]. In contrast, in the gastrodermis, the localized up-regulation of *GFP* expression and *GFP* fluorescence in the pseudo-bud structures was unexpected. Preliminary results indicate that the *RNAi*-induced decrease in *β-catenin* transcript levels leads to the rapid nuclear translocation of the *β-catenin* protein available in gastrodermal cells and the subsequent trans-activation of *β-catenin/TCF* target genes such as *Sp5*.

This paradoxal response to *β-catenin(RNAi)* explains (a) the rapid growth of pseudo-bud structures in starved animals that normally do not bud, (b) the high level of gastrodermal *Sp5-3169:GFP* and *Sp5* expression in these structures, (c) the lack of head structure differentiation due to the high level of *Sp5* and inhibition of the head organizer. This two-step response to *β-catenin* knock-down provides an experimental paradigm for inducing the proliferative phase of the budding process in the absence of apical differentiation and for characterizing the molecular players required in parental tissues.

#### 4.6. Variability of head organizer inhibitor strength across *Hydra* strains

In this study, we observed great phenotypic variability between *Hv\_Basel* and *Hv\_AEP2* after exposure to GRN modulators, whether ALP treatment or *Sp5* knockdown. After ALP, *Hv\_Basel* develop numerous ectopic tentacles along their body column within a few days, whereas *Hv\_AEP2* form very few, even after seven days of ALP exposure. In *Hv\_Basel*, a two-day exposure to ALP leads to a first wave of *Sp5* up-regulation, followed two days later by a second wave of *Wnt3* up-regulation inducing the formation of small *Wnt3* spots along the body column and the subsequent emergence of multiple ectopic tentacles as observed in *Hv\_ZiiL2*.

In non-transgenic *Hv\_AEP2* animals as well as in *Sp5-3169:GFP* and *Wnt3-2149:GFP* transgenic animals exposed to ALP, the two waves of gene regulation appear as in *Hv\_Basel* with a first transient up-regulation of *Sp5*, limited to several ectopic large circles in the epidermis and a more diffuse and intense expression in the gastrodermis. This is followed by the appearance of *Wnt3* spots along the body column, with just a few in the epidermis and multiple spots with *Wnt3* diffuse expression in the gastrodermis (Figure 8D,8E). Nevertheless, only rare ectopic tentacles do form. We infer that despite multiple spots of high

Wnt3, Sp5 activity is constitutively higher along the gastrodermis, repressing  $\beta$ -catenin that is kept minimal in SC2 epithelial stem cells. 1082  
1083

After *Sp5(RNAi)*, all *Hv\_Basel* animals become multiheaded, whereas *Hv\_AEP2* animals treated in the same way do not. This highly penetrant multiheaded phenotype in *Hv\_Basel* occurs without affecting the original head region, likely because *Sp5* expression remains high there, less subject to modulation sufficient to have a phenotypic impact (Figure 8B, 8C). By contrast, after *Sp5(RNAi)*, the body column acquires the properties of a head organizer. However, this does not happen in *Hv\_AEP2* animals where the absence of ectopic axis formation upon *Sp5(RNAi)* is explained by the fact that gastrodermal cells express *Sp5* at higher constitutive levels than in *Hv\_Basel*, maintaining *Sp5* repression on Wnt3 and  $\beta$ -catenin expression and preventing ectopic axis formation. 1084  
1085  
1086  
1087  
1088  
1089  
1090  
1091  
1092

In conclusion, the rarity of the ectopic tentacle phenotype after ALP or the absence of the multiple head phenotype after exposure to *Sp5(RNAi)* in *Hv\_AEP2* animals result from the stronger activity of the head organizer inhibitor along the body column in these animals compared to that present along the body column of *Hv\_Basel* or *Hv\_ZiiL2* animals. These results are consistent with previous studies that revealed, through systematic transplantation experiments performed on a variety of *Hydra* strains, significant variations in the respective strengths of the head activation and head inhibition components along the apical-to-basal axis between *Hydra* strains [63,64,6]. These results also highlight the predominant role of the gastrodermis in the negative regulation of the head organizer as previously demonstrated by producing chimeric animals with gastrodermal epithelial cells isolated from strains with low or high levels of head inhibition [65]. 1093  
1094  
1095  
1096  
1097  
1098  
1099  
1100  
1101  
1102  
1103

## 5. Conclusions

 1104

This study, based on the analysis of *Sp5* and *Wnt3* regulation in each epithelial layer of *Hydra*, reveals distinct architectures of the *Wnt3/β-catenin/TCF/Sp5/Zic4* GRN in different anatomical regions of the animal. Each architecture is characterized by a specific relative weight for each component, providing a unique combination that controls or prevents a specific patterning process. In the context of tentacle formation, the  $\beta$ -catenin dependent activation of a subset of the GRN, namely *Sp5* and *Zic4*, plays the leading role in the epidermis and the head activator component is kept inactive. In the context of head maintenance or head formation, the head activator component, i.e. *Wnt3/β-catenin/TCF* signaling, plays the leading role in the gastrodermis. In the context of the body column, the head inhibitor component plays the leading role in the gastrodermis to keep the head organizer locked, even though time- and space-restricted down-regulation of *Sp5* can occur, supporting the localized activation of *Wnt3/β-catenin/TCF* signaling and further ectopic head formation. 1105  
1106  
1107  
1108  
1109  
1110  
1111  
1112  
1113  
1114  
1115  
1116  
1117

The next step will be to compare the epidermal and gastrodermal chromatin signatures in the hypostome, the apical-regenerating tips, the tentacle ring, along the body column to map the regulatory sites linked to the context-specific GRN architecture. The complete set of actors involved in each context as well as the role they play in relation with the *Wnt3/β-catenin/TCF/Sp5/Zic4* GRN remains to be identified, e.g. Brachyury [66,67], MAPK/CREB [41,68,24,69,70] for head activation; notum [37], Dkk1/2/4, Thrombospondin, HAS7 [71–74] for head inhibition; *Alx* and Notch signaling for tentacle formation [75–77]. Also, further questions to investigate will be how this GRN that is conserved across evolution [32,62,33] moves from one architecture to another, typically when *Sp5* or  $\beta$ -catenin levels reach some threshold values or when additional players modify the GRN patterning function. More generally, an in-depth understanding of the molecular mechanisms behind the formation of the organizing center should enable us to transform a somatic tissue into one endowed with developmental organizing properties. 1118  
1119  
1120  
1121  
1122  
1123  
1124  
1125  
1126  
1127  
1128  
1129  
1130  
1131

<b>Supplementary Materials:</b> The following supporting information can be downloaded at: www.xxx,	1132
<b>Table S1:</b> Accession numbers of the <i>Hydra</i> genes used in this study;	1133
<b>Table S2:</b> List of primers, siRNAs and ds-oligonucleotides;	1134
<b>Table S3:</b> List of reporter or expression constructs used in this work;	1135
<b>Figure S1:</b> <i>Sp5</i> (t29291aep) single-cell expression as deduced from <i>Hydra</i> single-cell transcriptomes produced by Siebert et al (2019) and made available on <a href="#">Single Cell Portal</a> ;	1136
<b>Figure S2:</b> Map and sequences of the <i>HyActin-1388:mCherry_HySp5-3169:GFP</i> construct (10'533 bp) further named <i>HySp5-3169:GFP</i> construct;	1137
<b>Figure S3:</b> GFP and mCherry fluorescence in intact transgenic animals expressing the <i>HyActin-1388:mCherry_HySp5-3169:GFP</i> construct either in the epidermis or in the gastrodermis;	1138
<b>Figure S4:</b> GFP expression in regenerating epidermal and gastrodermal <i>HySp5-3169:GFP</i> animals;	1139
<b>Figure S5:</b> GFP and mCherry fluorescence in apical-regenerating (AR) or basal-regenerating (BR) halves of epidermal and gastrodermal <i>HySp5-3169:GFP</i> transgenic animals;	1140
<b>Figure S6:</b> Impact of alsterpaullone treatment on <i>Sp5</i> and <i>Wnt3</i> expression in <i>Hv_AEP2</i> animals;	1141
<b>Figure S7:</b> Impact of ALP treatment on <i>Sp5</i> , GFP and <i>Wnt3</i> expression in epidermal and gastrodermal <i>HySp5-3169:GFP</i> transgenic animals;	1142
<b>Figure S8:</b> Impact of ALP treatment on <i>GFP</i> , <i>Wnt3</i> and <i>Sp5</i> expression pattern in epidermal and gastrodermal <i>HyWnt3-2149:GFP</i> transgenic animals;	1143
<b>Figure S9:</b> Impact of $\beta$ -catenin(RNAi) on $\beta$ -catenin, <i>Sp5</i> and <i>GFP</i> transcript levels in epidermal and gastrodermal <i>HySp5-3169:GFP</i> transgenic animals;	1144
<b>Figure S10:</b> Impact of $\beta$ -catenin(RNAi) on pseudo-bud formation and <i>Sp5</i> expression;	1145
<b>Figure S11:</b> Impact of $\beta$ -catenin(RNAi) on GFP and mCherry fluorescence in epidermal and gastrodermal <i>HySp5-3169:GFP</i> transgenic animals;	1146
<b>Figure S12:</b> Impact of $\beta$ -catenin(RNAi) on GFP and mCherry immuno-detected patterns in epidermal and gastrodermal <i>HySp5-3169:GFP</i> transgenic animals;	1147
<b>Figure S13:</b> Impact of <i>Sp5</i> (RNAi) on <i>Sp5</i> , <i>GFP</i> and <i>Wnt3</i> expression levels in epidermal and gastrodermal <i>HySp5-3169:GFP</i> transgenic animals;	1148
<b>Figure S14:</b> Impact of <i>Sp5</i> (RNAi) on <i>GFP</i> expression in epidermal and gastrodermal <i>HySp5-3169:GFP</i> transgenic animals;	1149
<b>Figure S15:</b> Impact of <i>Sp5</i> (RNAi) on GFP and mCherry fluorescence in epidermal or gastrodermal <i>HySp5-3169:GFP</i> transgenic animals;	1150
<b>Figure S16:</b> Impact of <i>Sp5</i> (RNAi) on GFP fluorescence in epidermal and gastrodermal <i>HySp5-3169:GFP</i> animals;	1151
<b>Figure S17:</b> ChIP-qPCR analysis of the <i>Sp5</i> -binding sites in the <i>HySp5</i> promoter using anti <i>HySp5</i> antibodies;	1152
<b>Figure S18:</b> Mapping the putative <i>Sp5</i> Transcriptional Start Sites (TSS);	1153
<b>Figure S19:</b> Putative <i>Zic4</i> -binding sites in the <i>Wnt3</i> and <i>Zic4</i> genomic sequences from <i>Hm-105 Hydra</i>	1154
<b>Author Contributions:</b> Conceptualization: LIO, MCV, PG, BG; Methodology: LIO, PG, BG; Investigation: LIO, CP, MCV, PG; Visualization: LIO, CP, PG, MCV, BG; Funding acquisition: BG; Supervision & project administration: BG; Writing – original draft: LIO, BG; Writing – review & editing: BG.	1155
<b>Funding:</b> This work was supported by the Canton of Geneva, the Swiss National Science Foundation grants (31003_169930; 310030_189122). LIO was supported by an iGE3 doctoral fellowship, PG by an Excellence Scholarship for Foreign Scholars of the Swiss Government.	1156
<b>Institutional Review Board Statement:</b> Not applicable	1157
<b>Informed Consent Statement:</b> Not applicable	1158
<b>Data Availability Statement:</b> Data are contained within the article and Supplementary Materials.	1159
<b>Acknowledgments:</b> The authors thank Denis Benoni for animal care, Ariel Ruiz-i-Altaba and Charisios Tsairis for fruitful discussions on the project, Leo Beccari for excellent advice, Wanda Buzgariu for commenting on the manuscript and all members of the Galliot lab for discussions.	1160
<b>Conflicts of Interest:</b> The authors declare no conflicts of interest. The funders had no role in the design of the study; in the collection, analyses, or interpretation of data; in the writing of the manuscript; or in the decision to publish the results.	1161
	1162
	1163
	1164
	1165
	1166
	1167
	1168
	1169
	1170
	1171
	1172
	1173
	1174
	1175
	1176
	1177
	1178
	1179
	1180
	1181
	1182
	1183
	1184
	1185
	1186

## Appendix A

**Table A1:** Summary table listing the results obtained in the epidermis and gastrodermis of *HySp5-3169:GFP* transgenic animals

1187  
1188  
1189

Experimental conditions	Phenotype Tested gene	Epidermal <i>HySp5-3169:GFP</i> animals	Gastrodermal <i>HySp5-3169:GFP</i> animals	Figures supplement.
INTACT ANIMALS	<i>GFP</i> , <i>GFP fluo</i>	Hypostome: whole tentacle ring, tentacles	Hypostome: outer, basis tentacle ring, tentacles	1C, 1D
	<i>GFP protein</i>	BC: graded Apical to Basal	BC: high from 90% to 40%	1E-1L S3
REGENERATING ANIMALS	<i>GFP</i> , <i>GFP fluo</i>	Apical R: <i>GFP+</i> from 24 hpa <i>GFP+</i> in upper AR half Basal R: no <i>GFP</i> , no <i>GFP</i>	Apical R: <i>GFP+</i> from 8 hpa <i>GFP+</i> in upper AR half Basal R: <i>GFP+ 8-12 hpa</i> , then <i>GFP- GFP</i> along BR halves	2A, 2B 2C, 2D S4, S5
	<i>GFP fluo</i>	<b>GFP+ patch (st.1)</b> <i>GFP+</i> budding belt (st.3,4) <b>GFP+ bud (st. 5,6)</b> <b>GFP+ head (st.9)</b>	diffuse <i>GFP+ polyp</i> (st.3, 4) diffuse <i>GFP+ bud</i> (st.5, 6) <b>low boundary <i>GFP+ belt</i> (st. 6)</b> diffuse <i>GFP+ bud</i> (st.9)	2E-2H
Alsterpaullone (ALP) treatment	Morphological Phenotype	shortening of tentacles (4d) small transient ectopic structures along the BC (2d, 4d) basal disc refined after 4d, apical-like: <i>Wnt3+</i> , <i>Sp5+</i>		3B, 3D, S6, S7, S8
	<i>Sp5</i>	<i>Sp5</i> Loss of apical <i>Sp5</i> (4d) <i>Sp5</i> diffuse along BC <b><i>Sp5</i> spots in upper BC (2d)</b> <b><i>Sp5</i> ring above basal disc (2d)</b>	<i>Sp5</i> Loss of apical <i>Sp5</i> (4d) <i>Sp5</i> diffuse along BC (2d) <b>higher <i>Sp5</i> diffuse in lower BC (4d)</b>	3A-3C, S7A, S7B
	<i>Wnt3</i>	<i>Wnt3</i> lost at the head tip <i>Wnt3+</i> in tentacle roots (2d) <i>Wnt3+</i> dots along BC (4d) High <i>Wnt3</i> at basal pole (4d)	<i>Wnt3</i> lost at the head tip <i>Wnt3+</i> in tentacle roots (2d) <i>Wnt3+</i> dots along BC (4d) High <i>Wnt3</i> at basal pole (4d)	3A-3C, S7A, S7B
	<i>GFP</i>	<b><i>GFP+ spots in upper BC (2d)</i></b> <b><i>GFP+ ring above basal disc</i></b>	<i>GFP</i> Loss of <i>GFP</i> in tentacle ring <b><i>GFP</i> diffuse along BC + rings</b> <b><i>GFP</i> diffuse along lower BC</b>	3A-3C, S7A, S7B
	<i>GFP fluo</i>	<i>GFP</i> diffuse along BC (4d) high <i>GFP</i> in peduncle (7d)	<i>GFP fluo</i> Loss of apical <i>GFP fluo</i> (4d) <b><i>GFP fluo</i> in lower half (7d)</b>	3D, S7A, S7B
	Morphological Phenotype	Size reduction <b><i>Pseudo-buds: GFP-</i></b>	Size reduction <b><i>Pseudo-buds: GFP+</i></b>	4B, 4C, S11, S12
	<i>β-catenin</i>	Apical: 2x decrease BC: no change	Apical: 2x decrease BC: <b>2x decrease</b>	4A, S9
	<i>Sp5</i>	No specific response	BC: transient increase	4A, 4B, S9, S10
	<i>GFP</i>	Apical: ~4x decrease BC: ~4x decrease	Apical: transient increase BC: no specific response	4A, S9 (Specific response)
	<i>GFP pattern</i>	Apical areas = 0 Ectopic patches along BC	Progressive reduction along lower body column	4B, 4C, S11, S12
scramble si RNAs	<i>β-catenin</i>	NO STRESS RESPONSE BC: mild decrease < 2x	Apical, BC: steady increase BC: mild decrease < 2x	4A, S9 5A, S13
	<i>Sp5</i>	NO STRESS RESPONSE BC: transient decrease	NO STRESS RESPONSE BC: transient decrease	4A, 4B, S9, S10 5A, S13
	<i>GFP</i>	BC: increase > 2x BC: decrease ~2x	BC: decrease > -1.41x NO STRESS RESPONSE	4A, S9 5A, S13
	<i>GFP pattern</i>	BC: Increase	BC: Progressive decrease along BC	4B, 4C, S11, S12
	<i>Wnt3</i>	BC: increase > 2x	BC: increase > 2x	5A, S13
	Morphological Phenotype	No multiheaded phenotype up to 2d pEP2 in the <i>Hv_AEP2</i> transgenic animals		5B,5C,5E, S14-S16
<i>Sp5 (RNAi)</i>	<i>Sp5</i>	BC: increase < 2x pEP1, pEP2	BC: increase < 2x pEP2	5A, S13
	<i>Wnt3</i>	BC: transient increase 16h pEP2	No significant modulation	5A, S13
	<i>GFP / GFP</i>	<b>Apical: increase 2x – 4x pEP1 - pEP2, then reduced 2x 2d pEP2;</b> <b>BC: increase &gt; 4x then reduced ~2x 2d pEP2</b>	No significant modulation	5A, 5D, S13
	<i>GFP / GFP pattern</i>	<b>BC: Extended areas of <i>GFP/GFP</i> overexpression along the BC</b>	Ectopic <i>GFP</i> spots 2d pEP2 in lower BC and in tentacles	5B, 5C, 5E, S14, S15, S16
	<i>β-catenin</i>	BC: increased ~1.5x 2d pEP2	BC: increased ~1.5x 2d pEP2	5D

1190  
1191  
1192

## References

1. Galliot, B. Hydra, a fruitful model system for 270 years. *Int J Dev Biol* **2012**, *56*, 411–423, doi:10.1387/ijdb.120086bg. 1194
2. Browne, E.N. The Production of New Hydranths in Hydra by the Insertion of Small Grafts. *J Exp Zool* **1909**, *7*, 1–37. 1195
3. Yao, T. Studies on the Organizer Problem in Pelmatohydra Oligactis. I. The Induction Potency of the Implants and the Nature of the Induced Hydranth. *J Exp Biol* **1945**, *21*, 145–150. 1196
4. MacWilliams, H.K. Hydra Transplantation Phenomena and the Mechanism of Hydra Head Regeneration. II. Properties of the Head Activation. *Dev Biol* **1983**, *96*, 239–257. 1198
5. Broun, M.; Bode, H.R. Characterization of the Head Organizer in Hydra. *Development* **2002**, *129*, 875–884, doi:10.1242/dev.129.4.875. 1200
6. Shimizu, H. Transplantation Analysis of Developmental Mechanisms in Hydra. *Int J Dev Biol* **2012**, *56*, 463–472, doi:10.1387/ijdb.123498hs. 1202
7. Vogg, M.C.; Wenger, Y.; Galliot, B. How Somatic Adult Tissues Develop Organizer Activity. *Curr Top Dev Biol* **2016**, *96*, 391–414, doi:10.1016/bs.ctdb.2015.11.002. 1204
8. Vogg, M.C.; Galliot, B.; Tsiairis, C.D. Model Systems for Regeneration: *Hydra*. *Development* **2019**, *146*, dev177212, doi:10.1242/dev.177212. 1206
9. Spemann, H.; Mangold, H. Über Die Induktion von Embryonalanlagen Durch Implantation Artfremder Organisatoren. *Wilhem Roux's Arch Entw Mech* **1924**, *100*, 599–638. 1208
10. De Robertis, E.M.; Wessely, O.; Oelgeschlager, M.; Brizuela, B.; Pera, E.; Larrain, J.; Abreu, J.; Bachiller, D. Molecular Mechanisms of Cell-Cell Signaling by the Spemann-Mangold Organizer. *Int J Dev Biol* **2001**, *45*, 189–197. 1210
11. Tickle, C.; Summerbell, D.; Wolpert, L. Positional Signalling and Specification of Digits in Chick Limb Morphogenesis. *Nature* **1975**, *254*, 199–202, doi:10.1038/254199a0. 1212
12. Alvarado-Mallart, R.-M.; Martinez, S.; Lance-Jones, C.C. Pluripotentiality of the 2-Day-Old Avian Germinative Neuroepithelium. *Dev Biol* **1990**, *139*, 75–88, doi:10.1016/0012-1606(90)90280-V. 1214
13. Nakamura, H. Do CNS Anlagen Have Plasticity in Differentiation? Analysis in Quail-Chick Chimera. *Brain Research* **1990**, *511*, 122–128, doi:10.1016/0006-8993(90)90231-Y. 1216
14. Joubin, K.; Stern, C.D. Formation and Maintenance of the Organizer among the Vertebrates. *Int J Dev Biol* **2001**, *45*, 165–175. 1218
15. Anderson, C.; Stern, C.D. Organizers in Development. *Curr Top Dev Biol* **2016**, *117*, 435–454, doi:10.1016/bs.ctdb.2015.11.023. 1219
16. Nye, H.L.; Cameron, J.A.; Chernoff, E.A.; Stocum, D.L. Regeneration of the Urodele Limb: A Review. *Dev Dyn* **2003**, *226*, 280–294, doi:10.1002/dvdy.10236. 1220
17. Brockes, J.P.; Kumar, A. Comparative Aspects of Animal Regeneration. *Annu Rev Cell Dev Biol* **2008**, *24*, 525–549, doi:10.1146/annurev.cellbio.24.110707.175336. 1222
18. Kragl, M.; Knapp, D.; Nacu, E.; Khattak, S.; Maden, M.; Epperlein, H.H.; Tanaka, E.M. Cells Keep a Memory of Their Tissue Origin during Axolotl Limb Regeneration. *Nature* **2009**, *460*, 60–65, doi:10.1038/nature08152. 1224
19. Rand, H.W.; Bovard, J.F.; Minnich, D.E. Localization of Formative Agencies in Hydra. *Proc Natl Acad Sci U S A* **1926**, *12*, 565–570. 1226
20. MacWilliams, H.K. Hydra Transplantation Phenomena and the Mechanism of Hydra Head Regeneration. I. Properties of the Head Inhibition. *Dev Biol* **1983**, *96*, 217–238. 1228
21. Gierer, A.; Meinhardt, H. A Theory of Biological Pattern Formation. *Kybernetik* **1972**, *12*, 30–39. 1230
22. Hobmayer, B.; Rentzsch, F.; Kuhn, K.; Happel, C.M.; von Laue, C.C.; Snyder, P.; Rothbächer, U.; Holstein, T.W. WNT Signalling Molecules Act in Axis Formation in the Diploblastic Metazoan Hydra. *Nature* **2000**, *407*, 186–189, doi:10.1038/35025063. 1231
23. Broun, M.; Gee, L.; Reinhardt, B.; Bode, H.R. Formation of the Head Organizer in Hydra Involves the Canonical Wnt Pathway. *Development* **2005**, *132*, 2907–2916, doi:10.1242/dev.01848. 1233
24. Chera, S.; Ghila, L.; Dobretz, K.; Wenger, Y.; Bauer, C.; Buzgariu, W.; Martinou, J.-C.; Galliot, B. Apoptotic Cells Provide an Unexpected Source of Wnt3 Signaling to Drive Hydra Head Regeneration. *Dev Cell* **2009**, *17*, 279–289, doi:10.1016/j.devcel.2009.07.014. 1235
25. Lengfeld, T.; Watanabe, H.; Simakov, O.; Lindgens, D.; Gee, L.; Law, L.; Schmidt, H.A.; Ozbek, S.; Bode, H.; Holstein, T.W. Multiple Wnts Are Involved in Hydra Organizer Formation and Regeneration. *Dev Biol* **2009**, *330*, 186–199, doi:S0012-1606(09)00105-5 [pii] 10.1016/j.ydbio.2009.02.004. 1239
26. Gee, L.; Hartig, J.; Law, L.; Wittlieb, J.; Khalturin, K.; Bosch, T.C.; Bode, H.R. Beta-Catenin Plays a Central Role in Setting up the Head Organizer in Hydra. *Dev Biol* **2010**, *340*, 116–124, doi:10.1016/j.ydbio.2009.12.036. 1241
27. Nakamura, Y.; Tsiairis, C.D.; Özbe, S.; Holstein, T.W. Autoregulatory and Repressive Inputs Localize Hydra Wnt3 to the Head Organizer. *Proc Natl Acad Sci U S A* **2011**, *108*, 9137–9142, doi:10.1073/pnas.1018109108. 1243
28. Weidinger, G.; Thorpe, C.J.; Wuennenberg-Stapleton, K.; Ngai, J.; Moon, R.T. The Sp1-Related Transcription Factors Sp5 and Sp5-like Act Downstream of Wnt/Beta-Catenin Signaling in Mesoderm and Neuroectoderm Patterning. *Curr. Biol.* **2005**, *15*, 489–500, doi:10.1016/j.cub.2005.01.041. 1245
29. Thorpe, C.J.; Weidinger, G.; Moon, R.T. Wnt/Beta-Catenin Regulation of the Sp1-Related Transcription Factor Sp5l Promotes Tail Development in Zebrafish. *Development* **2005**, *132*, 1763–1772, doi:10.1242/dev.01733. 1248

30. Fujimura, N.; Vacik, T.; Machon, O.; Vlcek, C.; Scalabrin, S.; Speth, M.; Diep, D.; Krauss, S.; Kozmik, Z. Wnt-Mediated down-Regulation of Sp1 Target Genes by a Transcriptional Repressor Sp5. *J. Biol. Chem.* **2007**, *282*, 1225–1237, doi:10.1074/jbc.M605851200. 1250  
1251  
1252

31. Park, D.-S.; Seo, J.-H.; Hong, M.; Bang, W.; Han, J.-K.; Choi, S.-C. Role of Sp5 as an Essential Early Regulator of Neural Crest Specification in Xenopus. *Dev. Dyn.* **2013**, *242*, 1382–1394, doi:10.1002/dvdy.24034. 1253  
1254

32. Kennedy, M.W.; Chalamalasetty, R.B.; Thomas, S.; Garriock, R.J.; Jailwala, P.; Yamaguchi, T.P. Sp5 and Sp8 Recruit  $\beta$ -Catenin and Tcf1-Lef1 to Select Enhancers to Activate Wnt Target Gene Transcription. *Proc Natl Acad Sci U S A* **2016**, *113*, 3545–3550, doi:10.1073/pnas.1519994113. 1255  
1256  
1257

33. Vogg, M.C.; Beccari, L.; Iglesias Ollé, L.; Rampon, C.; Vriz, S.; Perruchoud, C.; Wenger, Y.; Galliot, B. An Evolutionarily-Conserved Wnt3/ $\beta$ -Catenin/Sp5 Feedback Loop Restricts Head Organizer Activity in Hydra. *Nat Commun* **2019**, *10*, 312, doi:10.1038/s41467-018-08242-2. 1258  
1259  
1260

34. Vogg, M.C.; Ferenc, J.; Buzgariu, W.C.; Perruchoud, C.; Sanchez, P.G.L.; Beccari, L.; Nuninger, C.; Le Cras, Y.; Delucinge-Vivier, C.; Papasaikas, P.; et al. The Transcription Factor Zic4 Promotes Tentacle Formation and Prevents Epithelial Transdifferentiation in Hydra. *Sci Adv* **2022**, *8*, eabo0694, doi:10.1126/sciadv.abo0694. 1261  
1262  
1263

35. Siebert, S.; Farrell, J.A.; Cazet, J.F.; Abeykoon, Y.; Primack, A.S.; Schnitzler, C.E.; Juliano, C.E. Stem Cell Differentiation Trajectories in Hydra Resolved at Single-Cell Resolution. *Science* **2019**, *365*, eaav9314, doi:10.1126/science.aav9314. 1264  
1265

36. Schenkelaars, Q.; Perez-Cortes, D.; Perruchoud, C.; Galliot, B. The Polymorphism of Hydra Microsatellite Sequences Provides Strain-Specific Signatures. *PLoS One* **2020**, *15*, e0230547, doi:10.1371/journal.pone.0230547. 1266  
1267

37. Wenger, Y.; Buzgariu, W.; Perruchoud, C.; Loichot, G.; Galliot, B. Generic and Context-Dependent Gene Modulations during Hydra Whole Body Regeneration. *BioRxiv* **2019**, 587147, doi:10.1101/587147. 1268  
1269

38. Madeira, F.; Pearce, M.; Tivey, A.R.N.; Basutkar, P.; Lee, J.; Edbali, O.; Madhusoodanan, N.; Kolesnikov, A.; Lopez, R. Search and Sequence Analysis Tools Services from EMBL-EBI in 2022. *Nucleic Acids Res* **2022**, *50*, W276–W279, doi:10.1093/nar/gkac240. 1270  
1271

39. Wittlieb, J.; Khalturin, K.; Lohmann, J.U.; Anton-Erxleben, F.; Bosch, T.C. Transgenic Hydra Allow in Vivo Tracking of Individual Stem Cells during Morphogenesis. *Proc Natl Acad Sci U S A* **2006**, *103*, 6208–6211, doi:10.1073/pnas.0510163103. 1272  
1273

40. Pfaffl, M.W. A New Mathematical Model for Relative Quantification in Real-Time RT-PCR. *Nucleic Acids Res* **2001**, *29*, 45e–445, doi:10.1093/nar/29.9.e45. 1274  
1275

41. Galliot, B.; Welschhof, M.; Schuckert, O.; Hoffmeister, S.; Schaller, H.C. The cAMP Response Element Binding Protein Is Involved in Hydra Regeneration. *Development* **1995**, *121*, 1205–1216, doi:10.1242/dev.121.4.1205. 1276  
1277

42. Suknovic, N.; Tomczyk, S.; Clevret, D.; Perruchoud, C.; Galliot, B. The ULK1 Kinase, a Necessary Component of the pro-Regenerative and Anti-Aging Machinery in Hydra. *Mech Ageing Dev* **2021**, *194*, 111414, doi:10.1016/j.mad.2020.111414. 1278  
1279

43. Corish, P.; Tyler-Smith, C. Attenuation of Green Fluorescent Protein Half-Life in Mammalian Cells. *Protein Eng* **1999**, *12*, 1035–1040, doi:10.1093/protein/12.12.1035. 1280  
1281

44. Harrison, S.M.; Houzelstein, D.; Dunwoodie, S.L.; Beddington, R.S. Sp5, a New Member of the Sp1 Family, Is Dynamically Expressed during Development and Genetically Interacts with Brachyury. *Dev Biol* **2000**, *227*, 358–372, doi:10.1006/dbio.2000.9878. 1282  
1283  
1284

45. Hatayama, M.; Aruga, J. Role of Zic Family Proteins in Transcriptional Regulation and Chromatin Remodeling. In *Zic family*; Aruga, J., Ed.; Advances in Experimental Medicine and Biology; Springer Singapore: Singapore, 2018; Vol. 1046, pp. 353–380 ISBN 978-981-10-7310-6. 1285  
1286  
1287

46. Aruga, J.; Yokota, N.; Hashimoto, M.; Furuichi, T.; Fukuda, M.; Mikoshiba, K. A Novel Zinc Finger Protein, Zic, Is Involved in Neurogenesis, Especially in the Cell Lineage of Cerebellar Granule Cells. *J Neurochem* **1994**, *63*, 1880–1890, doi:10.1046/j.1471-4159.1994.63051880.x. 1288  
1289  
1290

47. Ishiguro, A.; Inoue, T.; Mikoshiba, K.; Aruga, J. Molecular Properties of Zic4 and Zic5 Proteins: Functional Diversity within Zic Family. *Biochem Biophys Res Commun* **2004**, *324*, 302–307, doi:S0006-291X(04)02078-9 [pii] 10.1016/j.bbrc.2004.09.052. 1291  
1292

48. Okumura, K.; Hosoe, Y.; Nakajima, N. Zic1 Is a Transcriptional Repressor Through the Lamin A/C Promoter and Has an Intrinsic Repressive Domain. *J Health Sci* **2004**, *50*, 423–427, doi:10.1248/jhs.50.423. 1293  
1294

49. Ebert, P.J.; Timmer, J.R.; Nakada, Y.; Helms, A.W.; Parab, P.B.; Liu, Y.; Hunsaker, T.L.; Johnson, J.E. Zic1 Represses *Math1* Expression via Interactions with the *Math1* Enhancer and Modulation of *Math1* Autoregulation. *Development* **2003**, *130*, 1949–1959, doi:10.1242/dev.00419. 1295  
1296  
1297

50. Salero, E.; Pérez-Sen, R.; Aruga, J.; Giménez, C.; Zafra, F. Transcription Factors Zic1 and Zic2 Bind and Transactivate the Apolipoprotein E Gene Promoter. *J Biol Chem* **2001**, *276*, 1881–1888, doi:10.1074/jbc.M007008200. 1298  
1299

51. Yang, Y.; Hwang, C.K.; Junn, E.; Lee, G.; Mouradian, M.M. ZIC2 and Sp3 Repress Sp1-Induced Activation of the Human D Dopamine Receptor Gene. *J Biol Chem* **2000**, *275*, 38863–38869, doi:10.1074/jbc.M007906200. 1300  
1301

52. Sakurada, T.; Mima, K.; Kurisaki, A.; Sugino, H.; Yamauchi, T. Neuronal Cell Type-Specific Promoter of the  $\alpha$  CaM Kinase II Gene Is Activated by Zic2, a Zic Family Zinc Finger Protein. *Neurosci Res* **2005**, *53*, 323–330, doi:10.1016/j.neures.2005.08.001. 1302  
1303

53. Sanchez-Ferras, O.; Bernas, G.; Laberge-Perrault, E.; Pilon, N. Induction and Dorsal Restriction of Paired-Box 3 (Pax3) Gene Expression in the Caudal Neuroectoderm Is Mediated by Integration of Multiple Pathways on a Short Neural Crest Enhancer. *BBA Gene Reg Mec* **2014**, *1839*, 546–558, doi:10.1016/j.bbagrnm.2014.04.023. 1304  
1305  
1306

54. Zhu, P.; Wang, Y.; He, L.; Huang, G.; Du, Y.; Zhang, G.; Yan, X.; Xia, P.; Ye, B.; Wang, S.; et al. ZIC2-Dependent OCT4 Activation Drives Self-Renewal of Human Liver Cancer Stem Cells. *J Clin Invest* **2015**, *125*, 3795–3808, doi:10.1172/JCI81979. 1307  
1308

55. Zhu, L.; Harutyunyan, K.G.; Peng, J.L.; Wang, J.; Schwartz, R.J.; Belmont, J.W. Identification of a Novel Role of ZIC3 in Regulating Cardiac Development. *Hum Mol Genet* **2007**, *16*, 1649–1660, doi:10.1093/hmg/ddm106. 1309  
1310

56. Lim, L.S.; Hong, F.H.; Kunarso, G.; Stanton, L.W. The Pluripotency Regulator Zic3 Is a Direct Activator of the Nanog Promoter in ESCs. *Stem Cells* **2010**, *28*, 1961–1969, doi:10.1002/stem.527. 1311  
1312

57. Satow, R.; Nakamura, T.; Kato, C.; Endo, M.; Tamura, M.; Batori, R.; Tomura, S.; Murayama, Y.; Fukami, K. ZIC5 Drives Melanoma Aggressiveness by PDGFD-Mediated Activation of FAK and STAT3. *Cancer Res* **2017**, *77*, 366–377, doi:10.1158/0008-5472.CAN-16-0991. 1313  
1314  
1315

58. Yagi, K.; Satou, Y.; Satoh, N. A Zinc Finger Transcription Factor, ZicL, Is a Direct Activator of *Brachyury* in the Notochord Specification of *Ciona intestinalis*. *Development* **2004**, *131*, 1279–1288, doi:10.1242/dev.01011. 1316  
1317

59. Yagi, K.; Satoh, N.; Satou, Y. Identification of Downstream Genes of the Ascidian Muscle Determinant Gene Ci-Macho1. *Dev Biol* **2004**, *274*, 478–489, doi:10.1016/j.ydbio.2004.07.013. 1318  
1319

60. Sawada, K.; Fukushima, Y.; Nishida, H. Macho-1 Functions as Transcriptional Activator for Muscle Formation in Embryos of the Ascidian *Halocynthia roretzii*. *Gene Expr Patt* **2005**, *5*, 429–437, doi:10.1016/j.modgep.2004.09.003. 1320  
1321

61. Korinek, V.; Barker, N.; Morin, P.J.; Van Wichen, D.; De Weger, R.; Kinzler, K.W.; Vogelstein, B.; Clevers, H. Constitutive Transcriptional Activation by a  $\beta$ -Catenin-Tcf Complex in APC $^{-/-}$  Colon Carcinoma. *Science* **1997**, *275*, 1784–1787, doi:10.1126/science.275.5307.1784. 1322  
1323  
1324

62. Huggins, I.J.; Bos, T.; Gaylord, O.; Jessen, C.; Lonquich, B.; Puranen, A.; Richter, J.; Rossdam, C.; Brafman, D.; Gaasterland, T.; et al. The WNT Target SP5 Negatively Regulates WNT Transcriptional Programs in Human Pluripotent Stem Cells. *Nat Commun* **2017**, *8*, 1034, doi:10.1038/s41467-017-01203-1. 1325  
1326  
1327

63. Takano, J.; Sugiyama, T. Genetic Analysis of Developmental Mechanisms in Hydra. VIII. Head-Activation and Head-Inhibition Potentials of a Slow-Budding Strain (L4). *J Embryol Exp Morphol* **1983**, *78*, 141–168. 1328  
1329

64. Achermann, J.; Sugiyama, T. Genetic Analysis of Developmental Mechanisms in Hydra. X. Morphogenetic Potentials of a Regeneration-Deficient Strain (Reg-16). *Dev Biol* **1985**, *107*, 13–27. 1330  
1331

65. Takano, J.; Sugiyama, T. Genetic Analysis of Developmental Mechanisms in Hydra. XII. Analysis of Chimaeric Hydra Produced from a Normal and a Slow-Budding Strain (L4). *J Embryol Exp Morphol* **1984**, *80*, 155–173. 1332  
1333

66. Technau, U.; Bode, H.R. HyBra1, a Brachyury Homologue, Acts during Head Formation in Hydra. *Development* **1999**, *126*, 999–1010. 1334  
1335

67. Schwaiger, M.; Andrikou, C.; Dnyansagar, R.; Murguia, P.F.; Paganos, P.; Voronov, D.; Zimmermann, B.; Lebedeva, T.; Schmidt, H.A.; Genikhovich, G.; et al. An Ancestral Wnt-Brachyury Feedback Loop in Axial Patterning and Recruitment of Mesoderm-Determining Target Genes. *Nat Ecol Evol* **2022**, *6*, 1921–1939, doi:10.1038/s41559-022-01905-w. 1336  
1337  
1338

68. Kaloulis, K.; Chera, S.; Hassel, M.; Gauchat, D.; Galliot, B. Reactivation of Developmental Programs: The cAMP-Response Element-Binding Protein Pathway Is Involved in Hydra Head Regeneration. *Proc Natl Acad Sci U S A* **2004**, *101*, 2363–2368. 1339  
1340

69. Chera, S.; Ghila, L.; Wenger, Y.; Galliot, B. Injury-Induced Activation of the MAPK/CREB Pathway Triggers Apoptosis-Induced Compensatory Proliferation in Hydra Head Regeneration: MAPK-Dependent Injury-Induced Apoptosis in Hydra. *Dev Growth Diff* **2011**, *53*, 186–201, doi:10.1111/j.1440-169X.2011.01250.x. 1341  
1342  
1343

70. Tursch, A.; Bartsch, N.; Mercker, M.; Schlüter, J.; Lommel, M.; Marciniak-Czochra, A.; Özbe, S.; Holstein, T.W. Injury-Induced MAPK Activation Triggers Body Axis Formation in *Hydra* by Default Wnt Signaling. *Proc Natl Acad Sci U S A* **2022**, *119*, e2204122119, doi:10.1073/pnas.2204122119. 1344  
1345  
1346

71. Guder, C.; Pinho, S.; Nacak, T.G.; Schmidt, H.A.; Hobmayer, B.; Niehrs, C.; Holstein, T.W. An Ancient Wnt-Dickkopf Antagonism in Hydra. *Development* **2006**, *133*, 901–911. 1347  
1348

72. Augustin, R.; Franke, A.; Khalurin, K.; Kiko, R.; Siebert, S.; Hemmrich, G.; Bosch, T.C. Dickkopf Related Genes Are Components of the Positional Value Gradient in Hydra. *Dev Biol* **2006**, *296*, 62–70, doi:S0012-1606(06)00283-1 [pii] 10.1016/j.ydbio.2006.04.003. 1349  
1350

73. Lommel, M.; Strompen, J.; Hellewell, A.L.; Balasubramanian, G.P.; Christofidou, E.D.; Thomson, A.R.; Boyle, A.L.; Woolfson, D.N.; Puglisi, K.; Hartl, M.; et al. Hydra Mesoglea Proteome Identifies Thrombospondin as a Conserved Component Active in Head Organizer Restriction. *Sci Rep* **2018**, *8*, 11753, doi:10.1038/s41598-018-30035-2. 1351  
1352  
1353

74. Ziegler, B.; Yiallouros, I.; Trageser, B.; Kumar, S.; Mercker, M.; Kling, S.; Fath, M.; Warnken, U.; Schnölzer, M.; Holstein, T.W.; et al. The Wnt-Specific Astacin Proteinase HAS-7 Restricts Head Organizer Formation in Hydra. *BMC Biol* **2021**, *19*, 120, doi:10.1186/s12915-021-01046-9. 1354  
1355  
1356

75. Smith, K.M.; Gee, L.; Bode, H.R. HyAlx, an Aristaless-Related Gene, Is Involved in Tentacle Formation in Hydra. *Development* **2000**, *127*, 4743–4752. 1357  
1358

76. Munder, S.; Tischer, S.; Grundhuber, M.; Buchels, N.; Bruckmeier, N.; Eckert, S.; Seefeldt, C.A.; Prexl, A.; Kasbauer, T.; Bottger, A. Notch-Signalling Is Required for Head Regeneration and Tentacle Patterning in Hydra. *Dev Biol* **2013**, *383*, 146–157, doi:10.1016/j.ydbio.2013.08.022. 1359  
1360  
1361

77. Pan, Q.; Mercker, M.; Klimovich, A.; Wittlieb, J.; Marciniak-Czochra, A.; Böttger, A. Genetic Interference with HvNotch Provides New Insights into the Role of the Notch-Signalling Pathway for Developmental Pattern Formation in Hydra. *Sci Rep* **2024**, *14*, 8553, doi:10.1038/s41598-024-58837-7. 1362  
1363  
1364  
1365